Electronic Supplementary Information for:

NHC-ligated Indenyl- and Fluorenyl-substituted Alanes and Gallanes: Synthons towards Indenyl- and Fluorenyl-bridged $(AlC)_n$-heterocycles (n = 2,3)

Luis Werner[a], Julika Hagn,[a] Alexander Gerstner,[a] and Udo Radius[a]*.

[a]Institut für Anorganische Chemie, Julius-Maximilians-Universität Würzburg, Am Hubland, 97074 Würzburg, Germany.

Content:

1) NMR spectra of compounds

(I*i*Pr^{Me})·AlH$_2$Ind **1**:

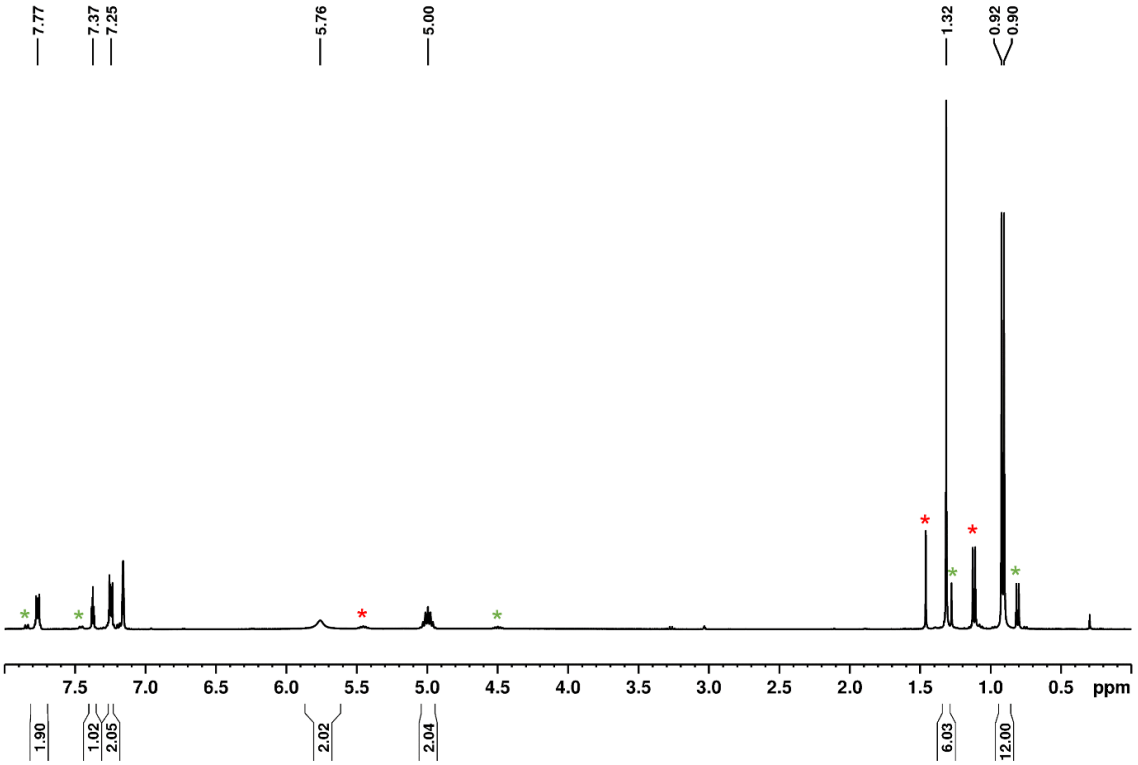

Figure S1. ^{1}H NMR spectrum (400.1 MHz, C_6D_6, 298 K) of (I*i*Pr^{Me})·AlH$_2$Ind **1** ((I*i*Pr^{Me})·AlH$_3$ marked with red asterisks, (I*i*Pr^{Me})·AlHInd$_2$ **13** marked with green asterisks).[S1]

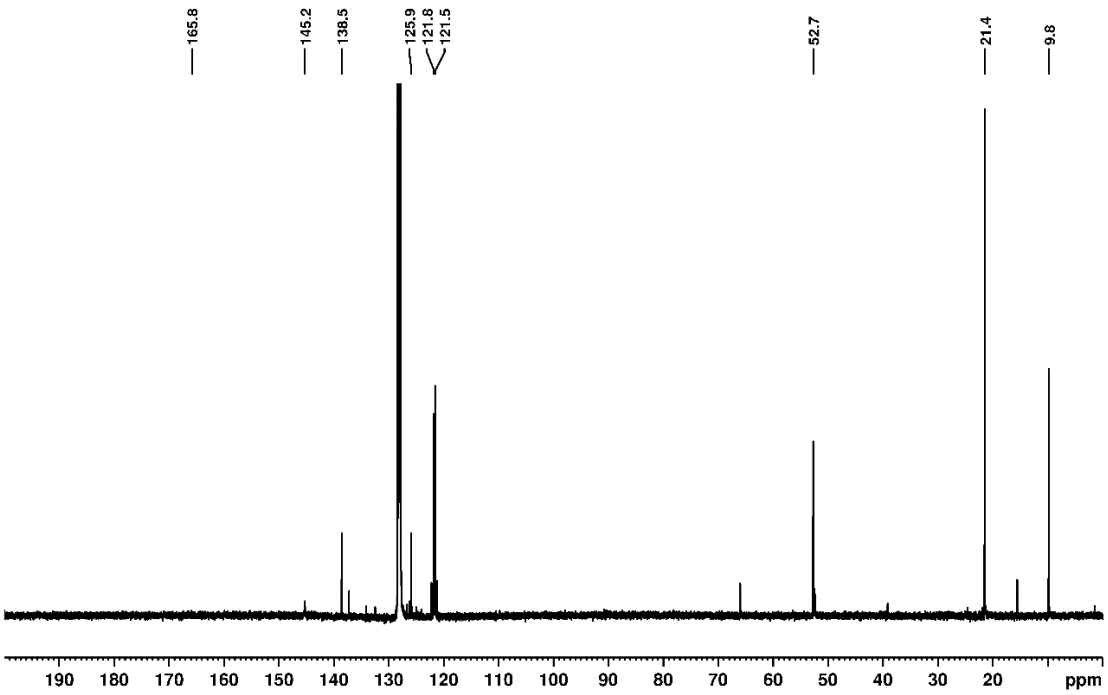

Figure S2. ^{13}C NMR spectrum (100.6 MHz, C_6D_6, 298 K) of (I*i*Pr^{Me})·AlH$_2$Ind **1.**

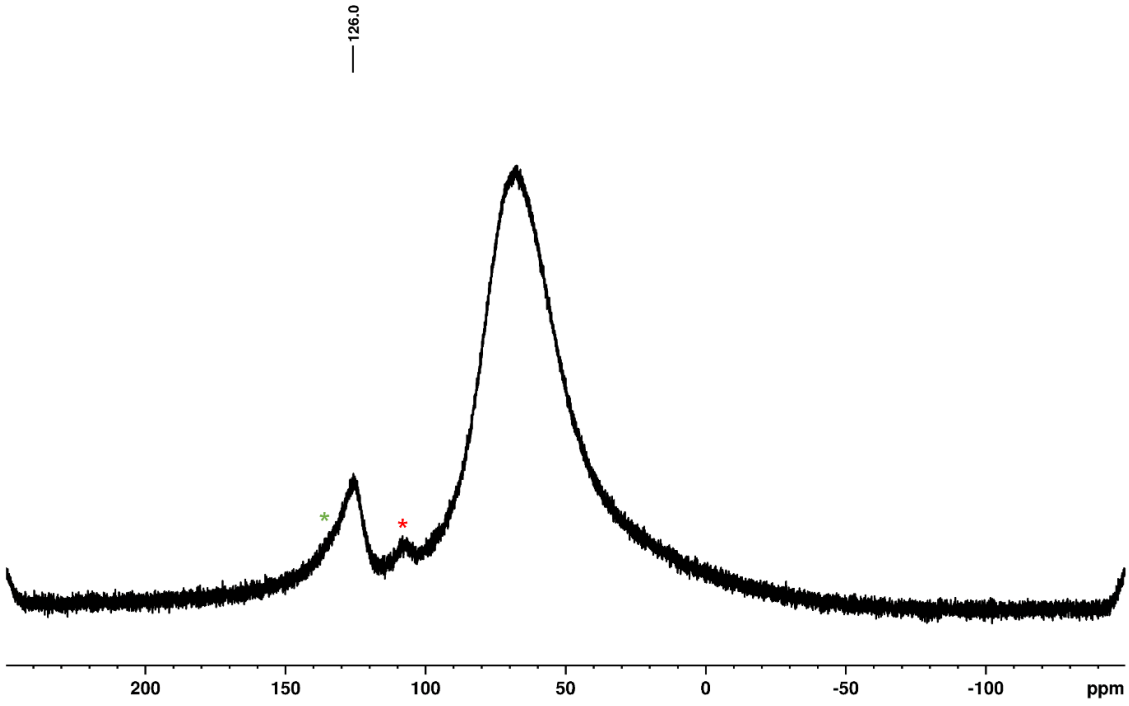

Figure S3. ^{27}Al NMR spectrum (104.3 MHz, C_6D_6, 298 K) of (I*i*Pr^{Me})·AlH_2Ind **1**((I*i*Pr^{Me})·AlH_3 marked with red asterisks, (I*i*Pr^{Me})·$AlHInd_2$ **13** marked with green asterisks)**.** [S1]

(I*i*Pr)·AlH_2Ind **2**:

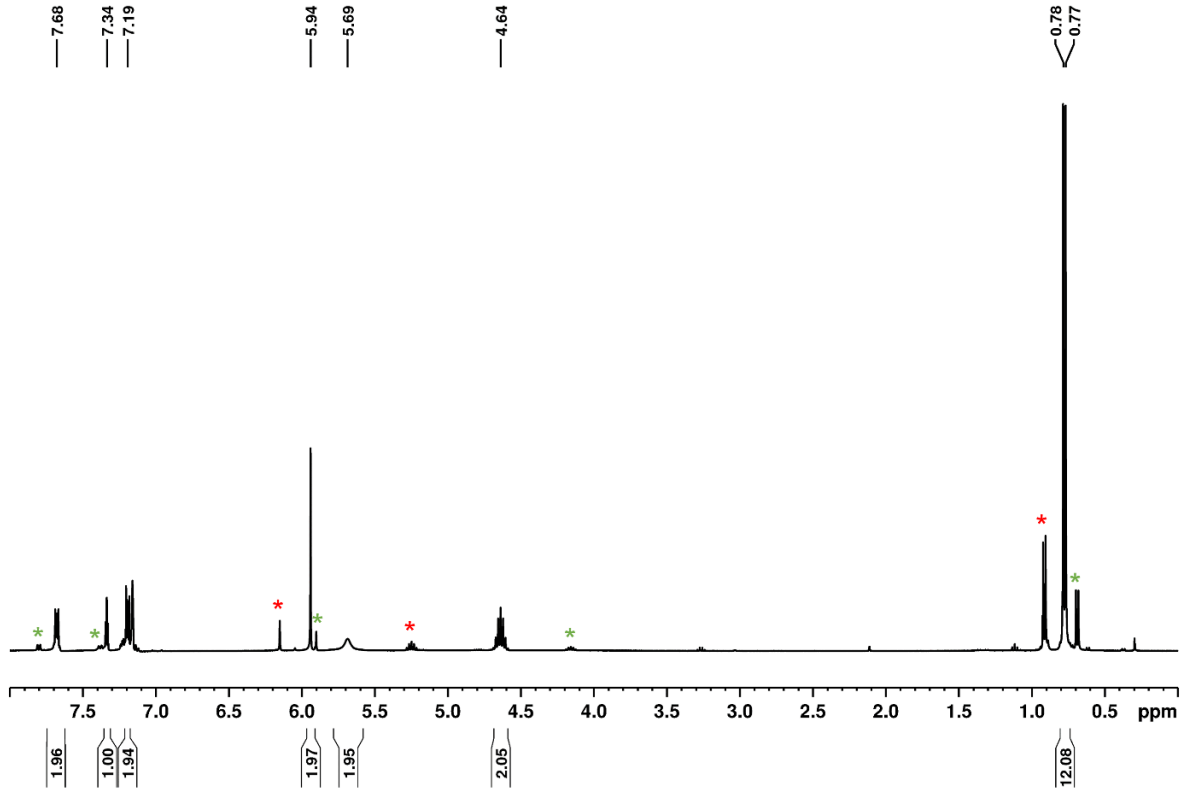

Figure S4. ^{1}H NMR spectrum (400.1 MHz, C_6D_6, 298 K) of (I*i*Pr)·AlH_2Ind **2** ((I*i*Pr)·AlH_3 marked with red asterisks, (I*i*Pr)·$AlHInd_2$ **14** marked with green asterisks)**.** [S1]

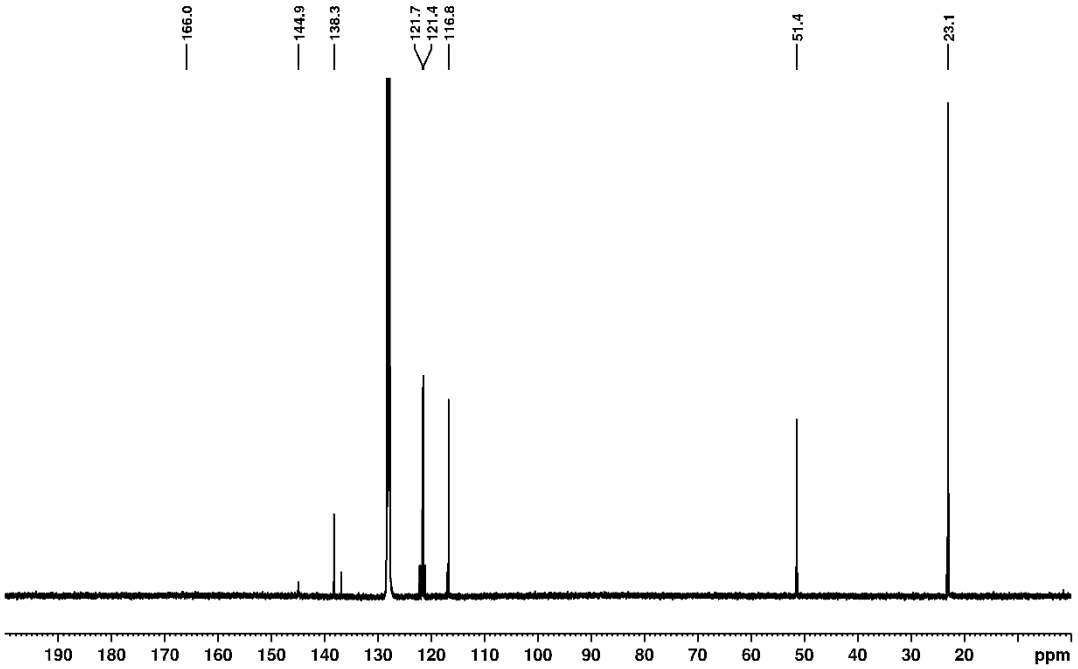

Figure S5. ^{13}C NMR spectrum (100.6 MHz, C_6D_6, 298 K) of (I*i*Pr)·AlH_2Ind **2**.

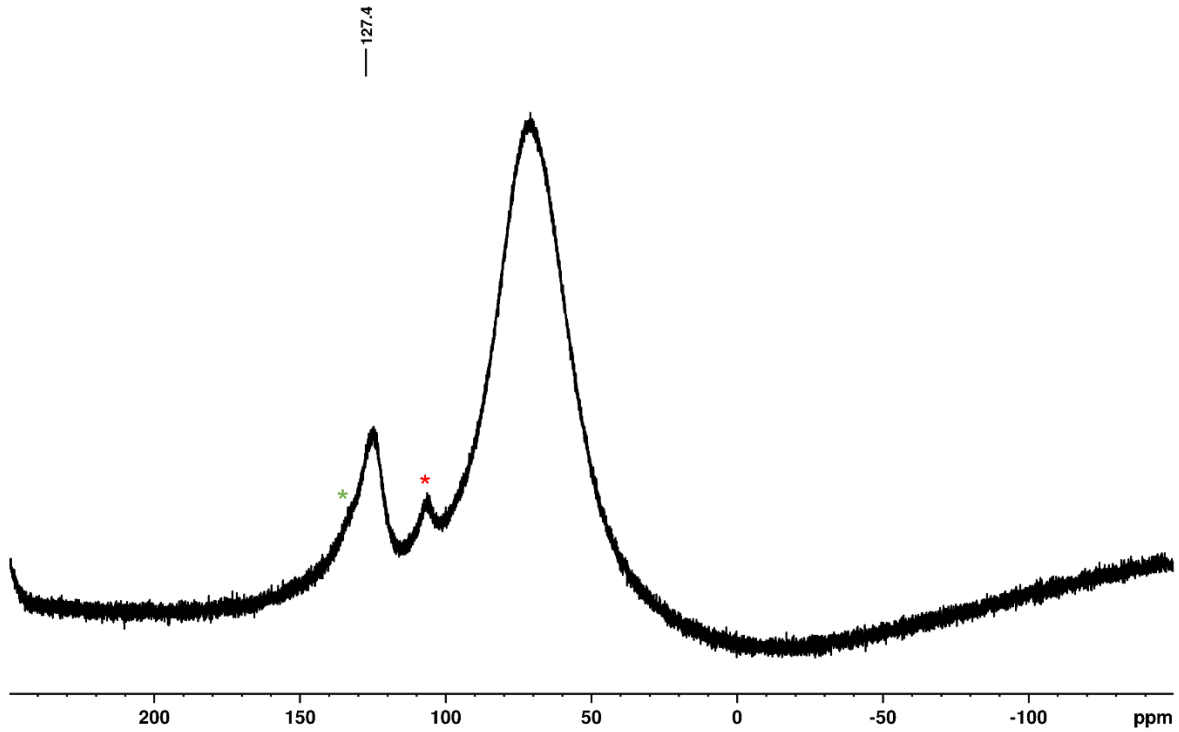

Figure S6. ^{27}Al NMR spectrum (104.3 MHz, C_6D_6, 298 K) of (I*i*Pr)·AlH_2Ind **2** ((I*i*Pr)·AlH_3 marked with red asterisks, (I*i*Pr)·$AlHInd_2$ **14** marked with green asterisks)**.** [S1]

(IMe^{Me})·AlH_2Ind **3**:

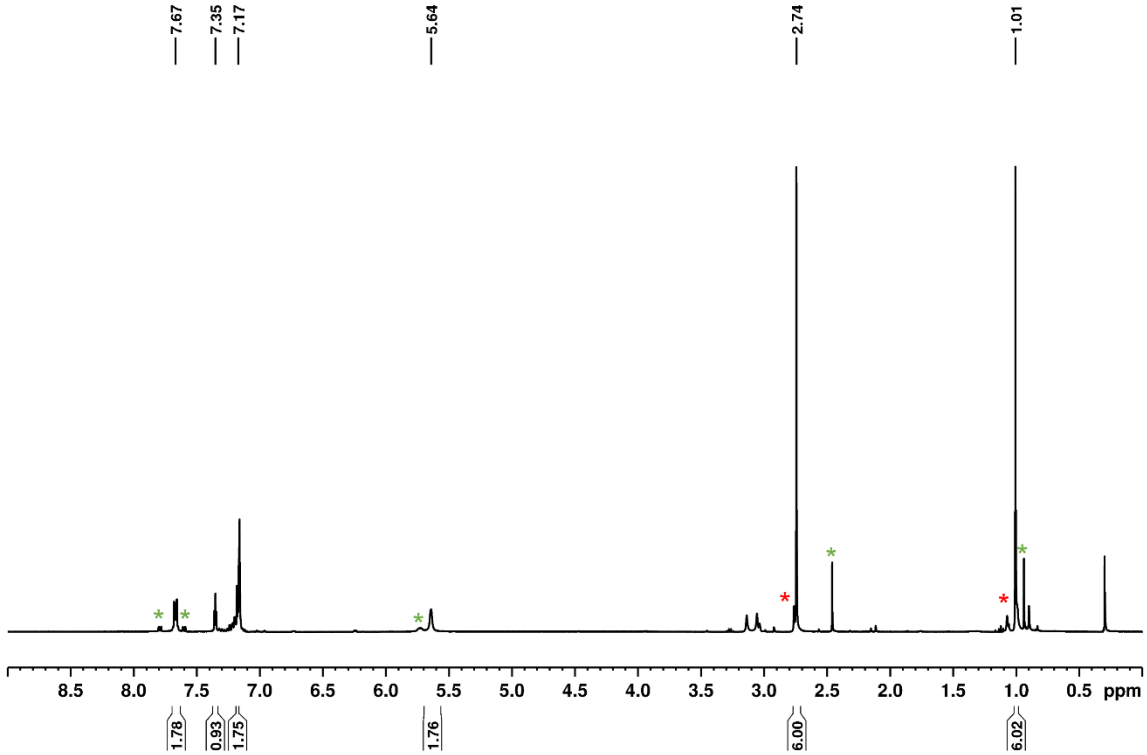

Figure S7. ^{1}H NMR spectrum (400.1 MHz, C_6D_6, 298 K) of (IMe^{Me})·AlH_2Ind **3** ((IMe^{Me})·AlH_3 marked with red asterisks, (IMe^{Me})·$AlHInd_2$ **15** marked with green asterisks)**.** [S1]

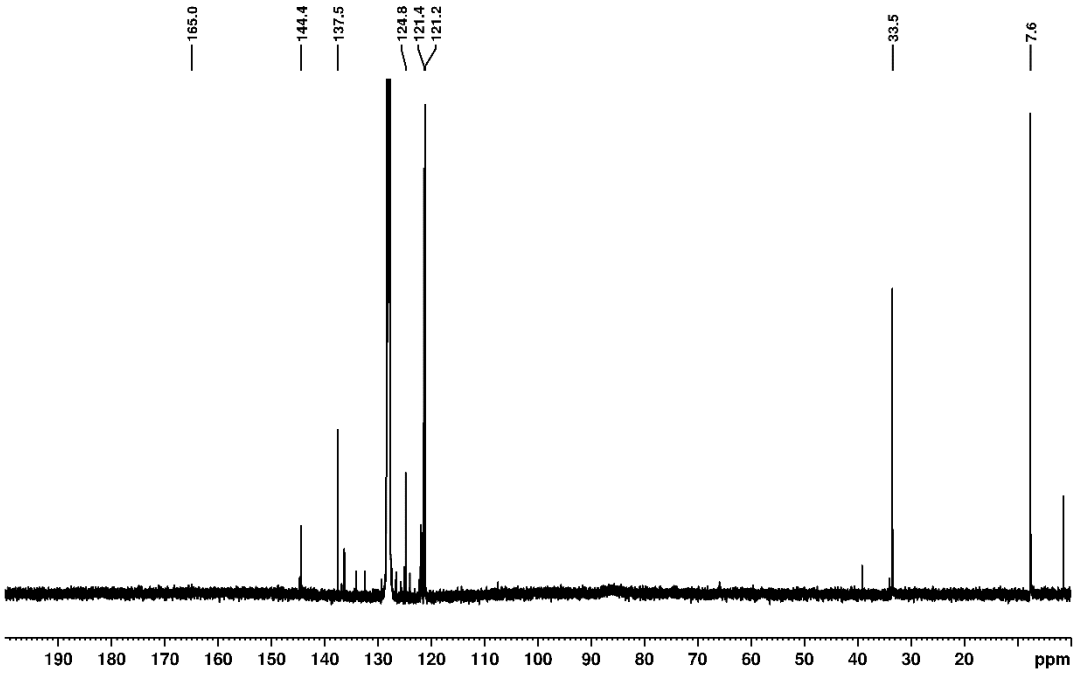

Figure S8. ^{13}C NMR spectrum (100.6 MHz, C_6D_6, 298 K) of (IMe^{Me})·AlH_2Ind **3.**

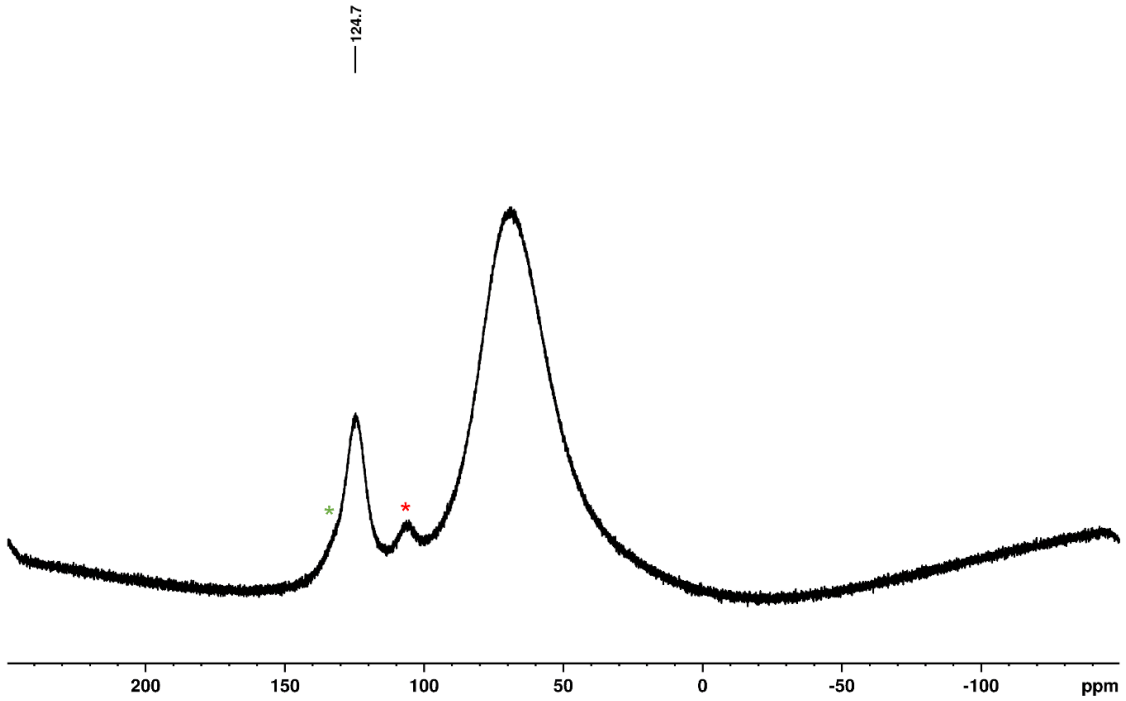

Figure S9. ^{27}Al NMR spectrum (104.3 MHz, C_6D_6, 298 K) of (IMe^{Me})·AlH_2Ind **3** ((IMe^{Me})·AlH_3 marked with red asterisks, (IMe^{Me})·$AlHInd_2$ **15** marked with green asterisks)**.** [S1]

(I*i*Pr^{Me})·AlH_2Fl **4**:

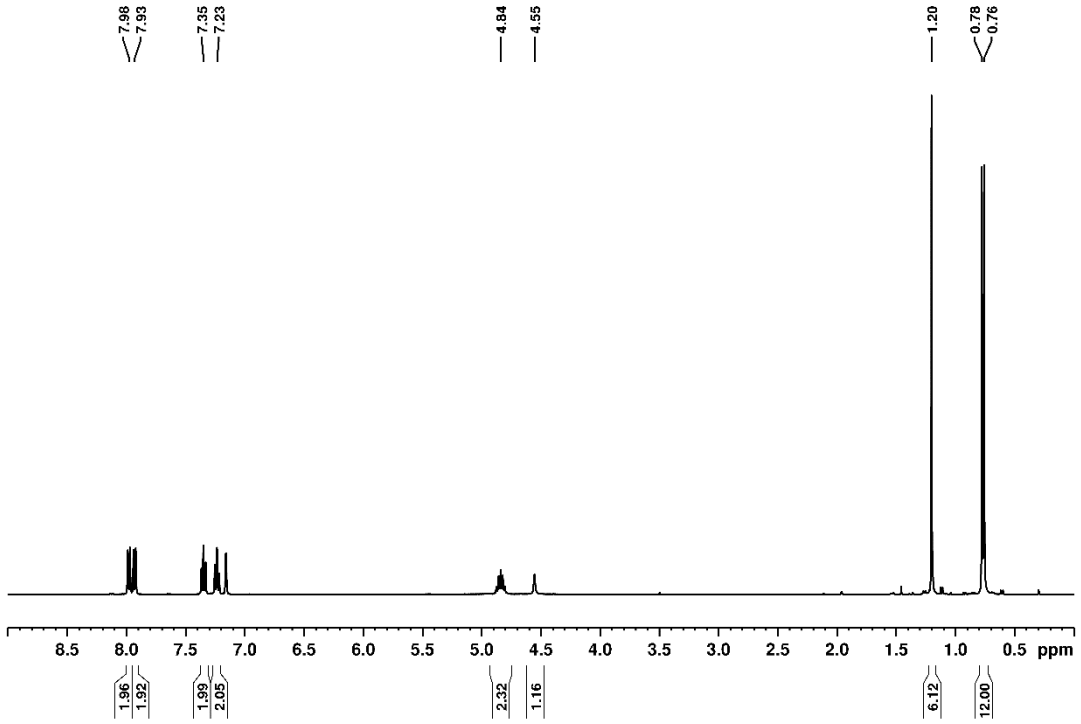

Figure S10. ^{1}H NMR spectrum (400.1 MHz, C_6D_6, 298 K) of (I*i*Pr^{Me})·AlH_2Fl **4**.

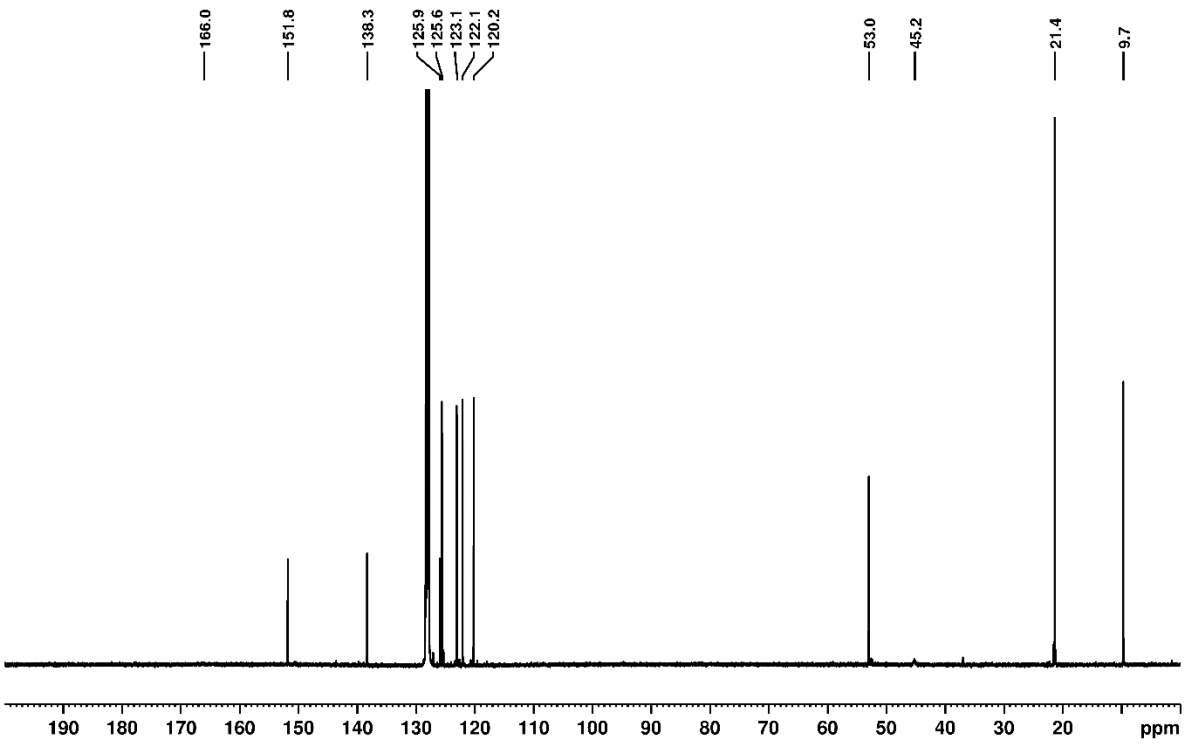

Figure S11. ^{13}C NMR spectrum (100.6 MHz, C_6D_6, 298 K) of (I*i*Pr^{Me})·AlH_2Fl **4**.

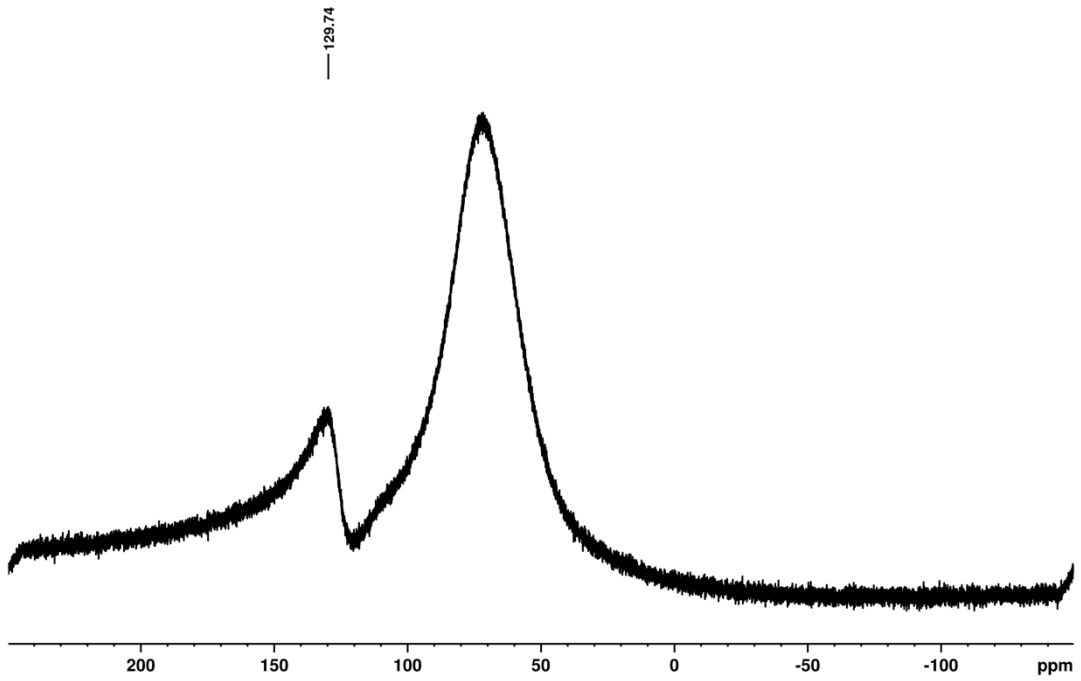

Figure S12. ^{27}Al NMR spectrum (104.3 MHz, C_6D_6, 298 K) of (I*i*Pr^{Me})·AlH_2Fl **4**.

(I*i*Pr)·AlH$_2$Fl **5:**

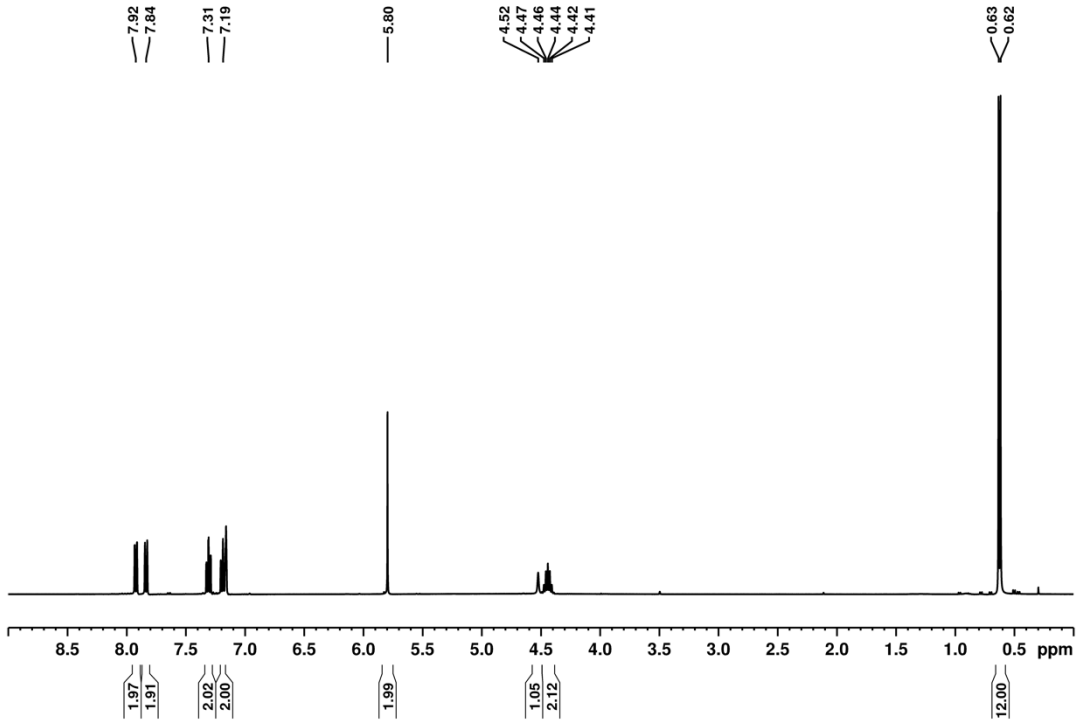

Figure S13. ^{1}H NMR spectrum (400.1 MHz, C_6D_6, 298 K) of (I*i*Pr)·AlH$_2$Fl **5**.

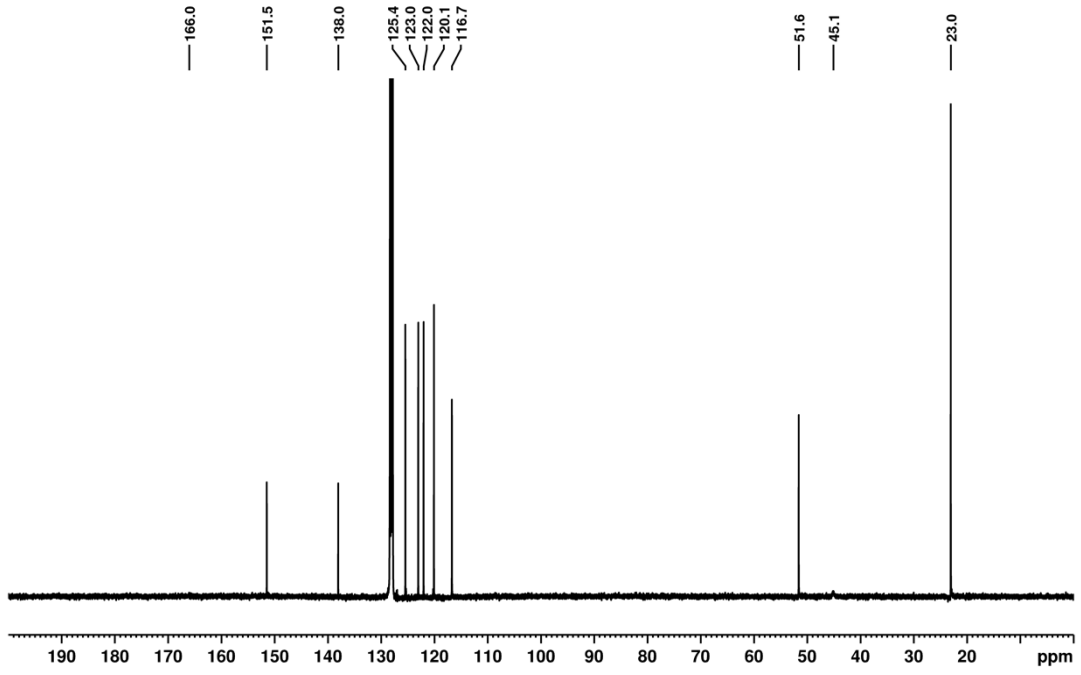

Figure S14. ^{13}C NMR spectrum (100.6 MHz, C_6D_6, 298 K) of (I*i*Pr)·AlH$_2$Fl **5**.

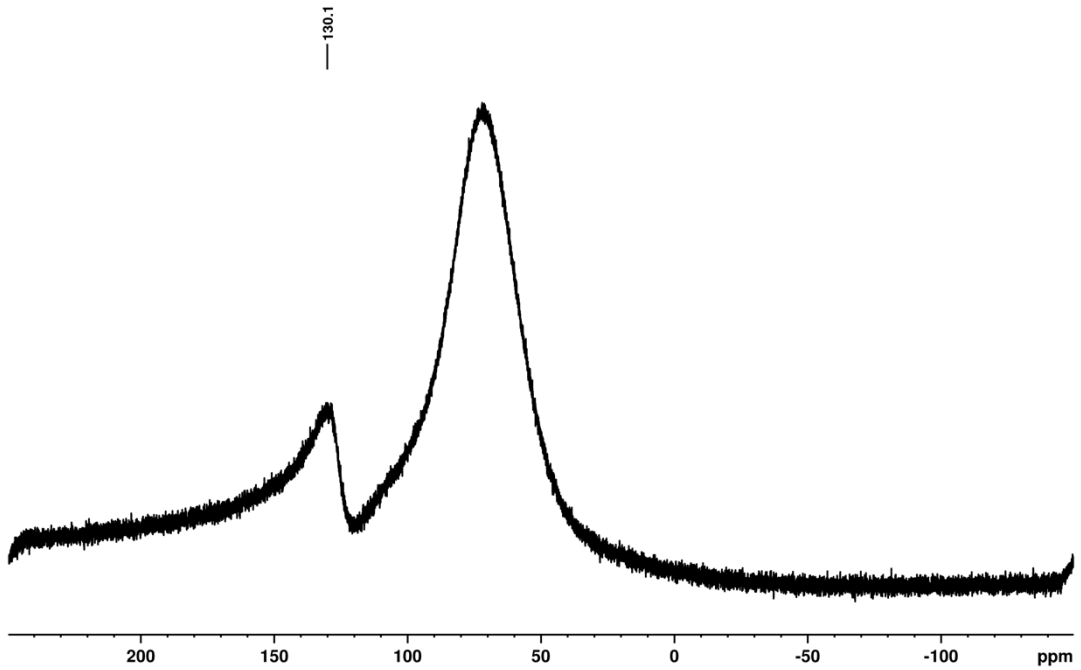

Figure S15. ^{27}Al NMR spectrum (104.3 MHz, C_6D_6, 298 K) of (I*i*Pr)·AlH_2Fl **5.**

(IMe^{Me})·AlH_2Fl **6**:

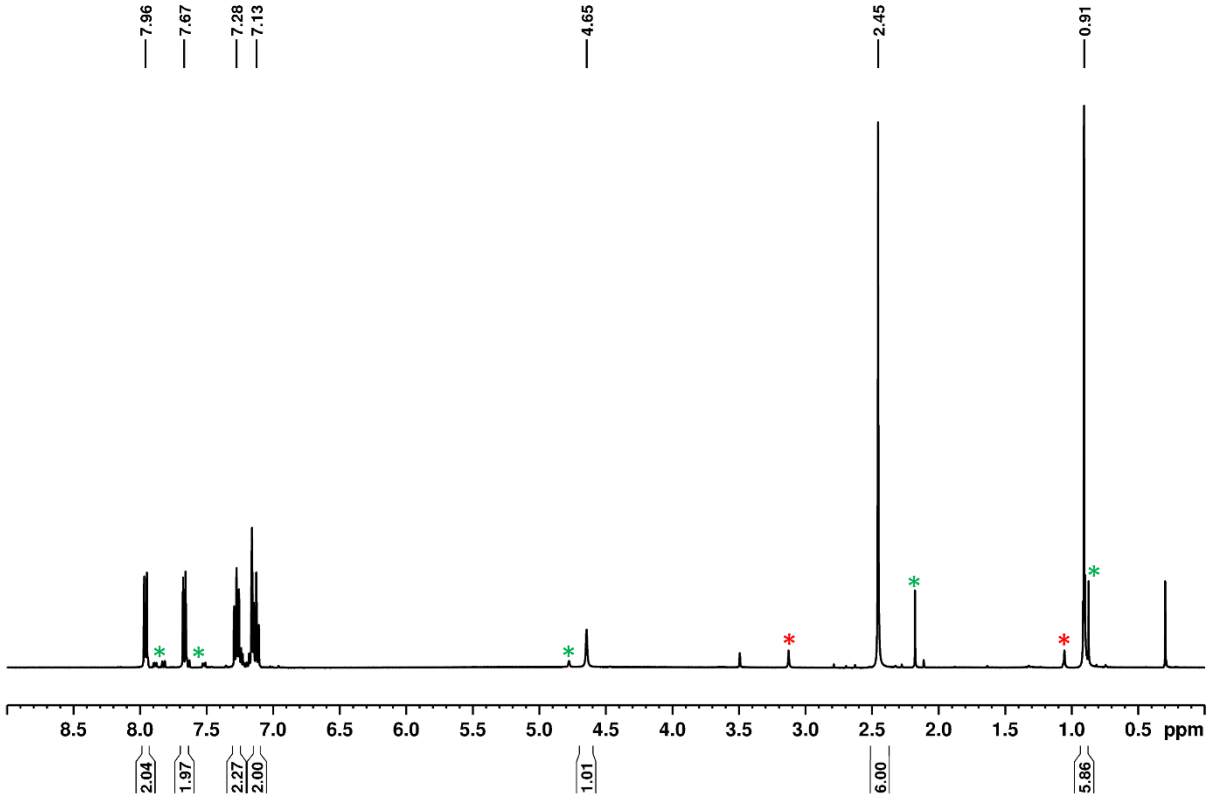

Figure S16. ^{1}H NMR spectrum (400.1 MHz, C_6D_6, 298 K) of (IMe^{Me})·AlH_2Fl **6** ((IMe^{Me})·AlH_3 marked with red asterisks, (IMe^{Me})·$AlHFl_2$ **18** marked with green asterisks).

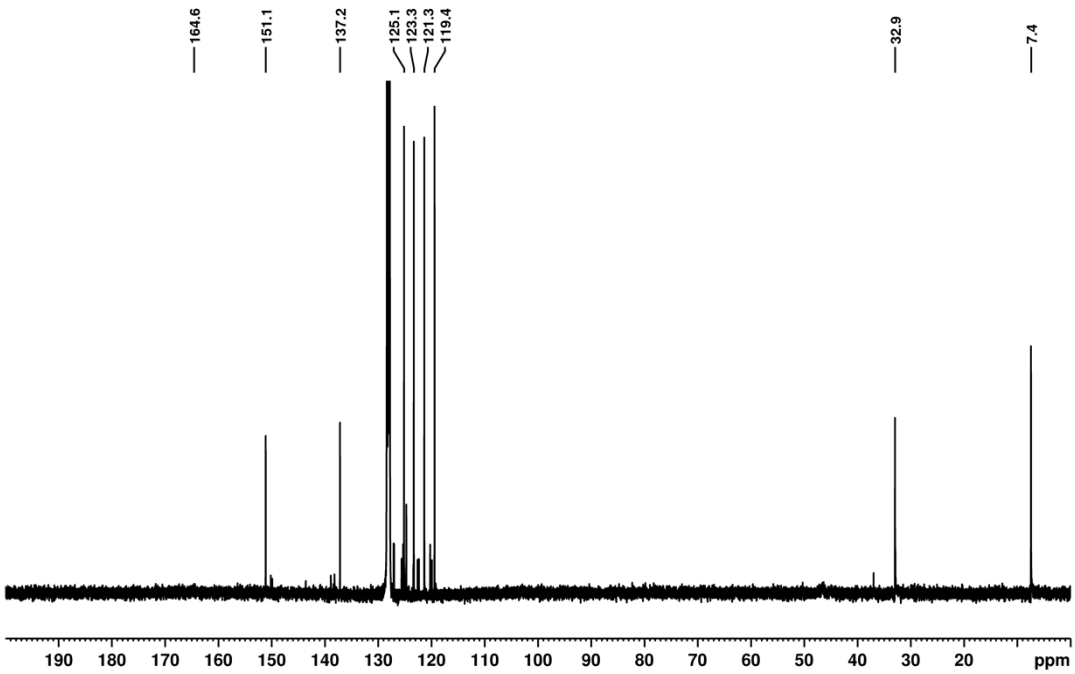

Figure S17. ^{13}C NMR spectrum (100.6 MHz, C_6D_6, 298 K) of (IMe^{Me})·AlH_2Fl **6.**

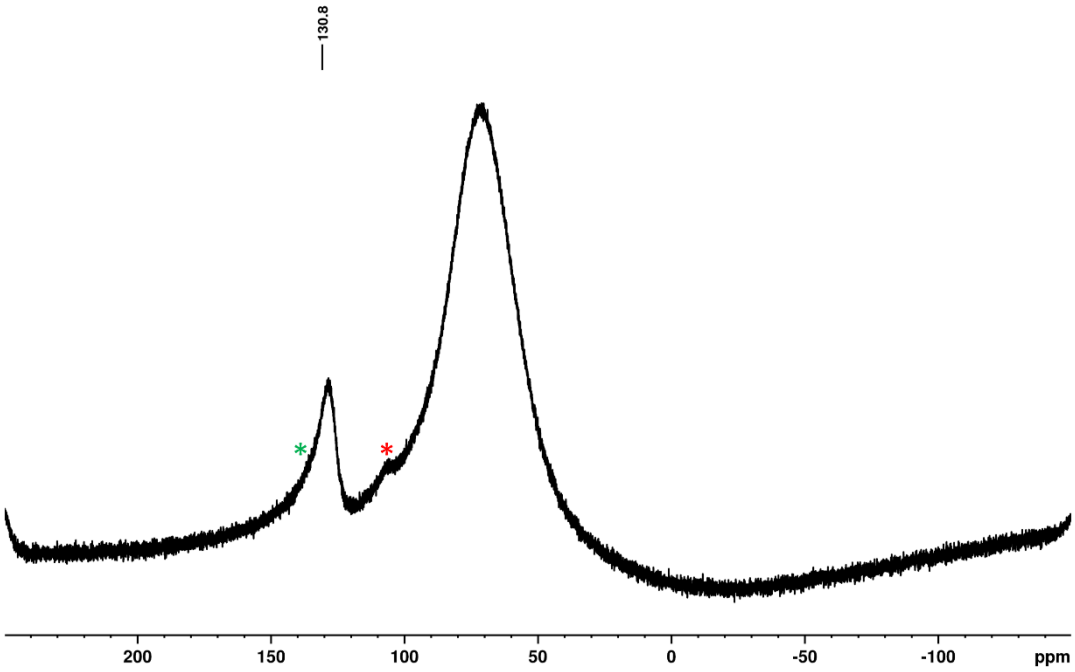

Figure S18. ^{27}Al NMR spectrum (104.3 MHz, C_6D_6, 298 K) of (IMe^{Me})·AlH_2Fl **6** ((IMe^{Me})·AlH_3 marked with red asterisks, (IMe^{Me})·$AlHFl_2$ **18** marked with green asterisks).

(I*i*Pr^{Me})·GaH$_2$Ind **7**:

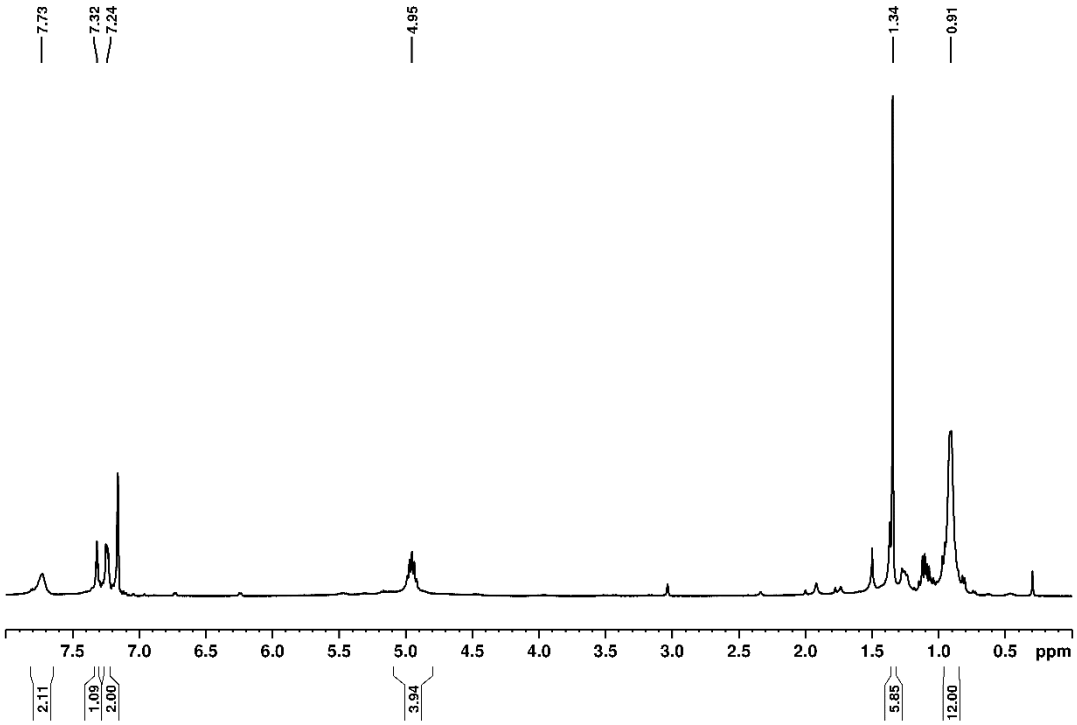

Figure S19. ^{1}H NMR spectrum (400.1 MHz, C_6D_6, 298 K) of (I*i*Pr^{Me})·GaH$_2$Ind **7** (unmarked signals belong to unknown impurities).

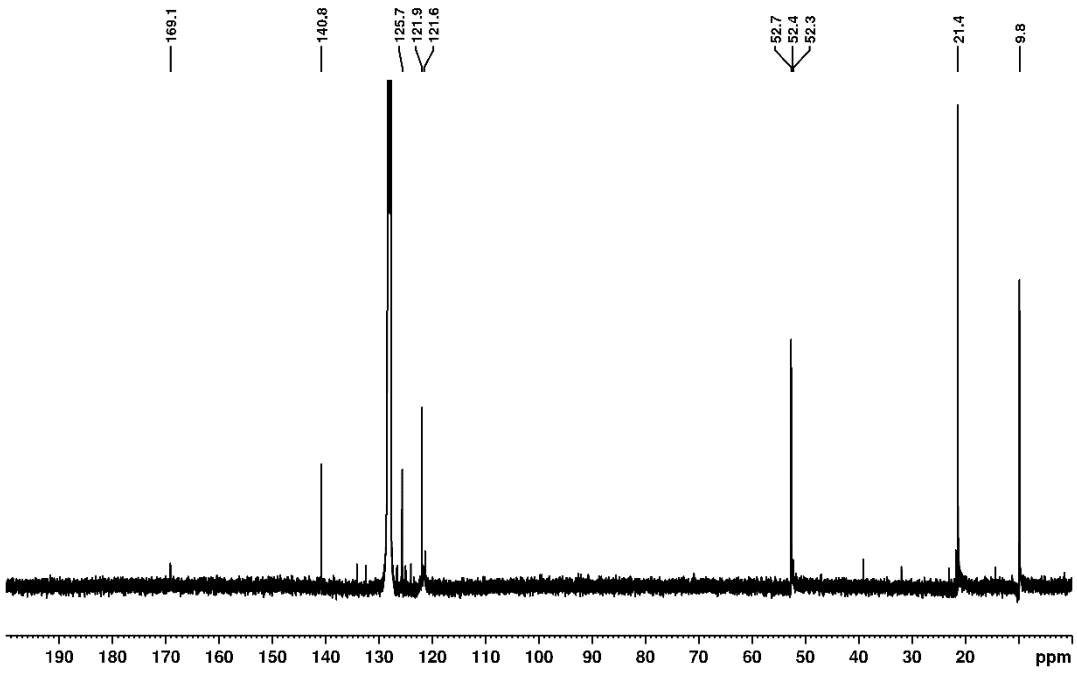

Figure S20. ^{13}C NMR spectrum (100.6 MHz, C_6D_6, 298 K) of (I*i*Pr^{Me})·GaH$_2$Ind **7**.

(I*i*Pr)·GaH$_2$Ind **8**:

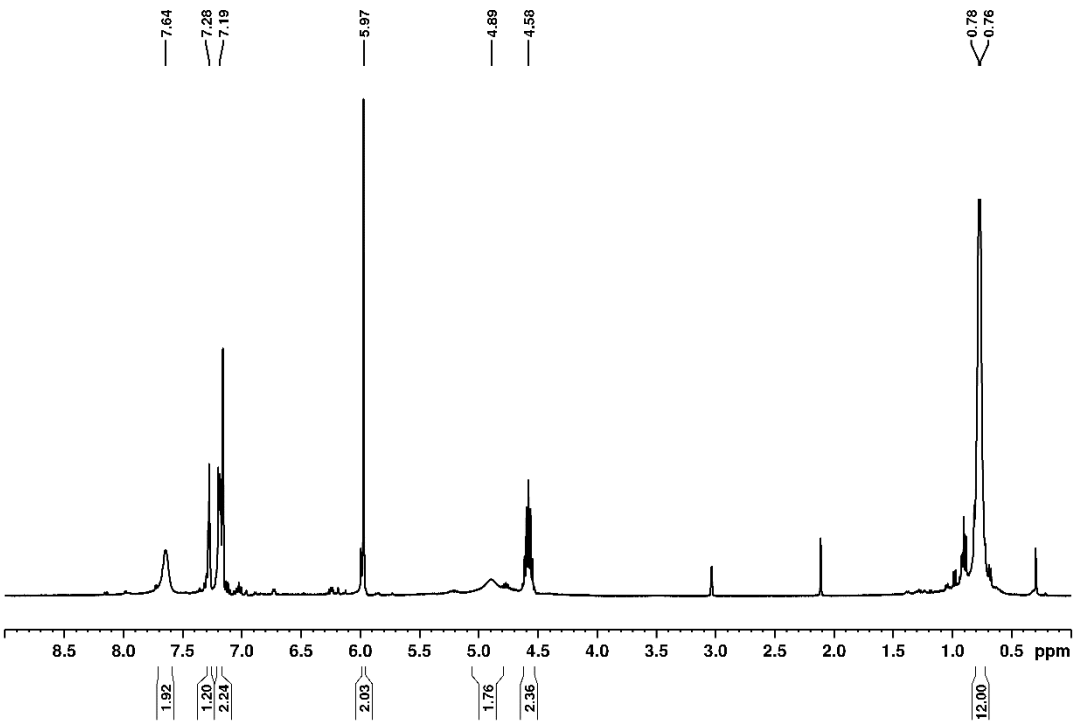

Figure S21. ^{1}H NMR spectrum (400.1 MHz, C_6D_6, 298 K) of (I*i*Pr)·GaH_2Ind **8** (unmarked signals belong to unknown impurities).

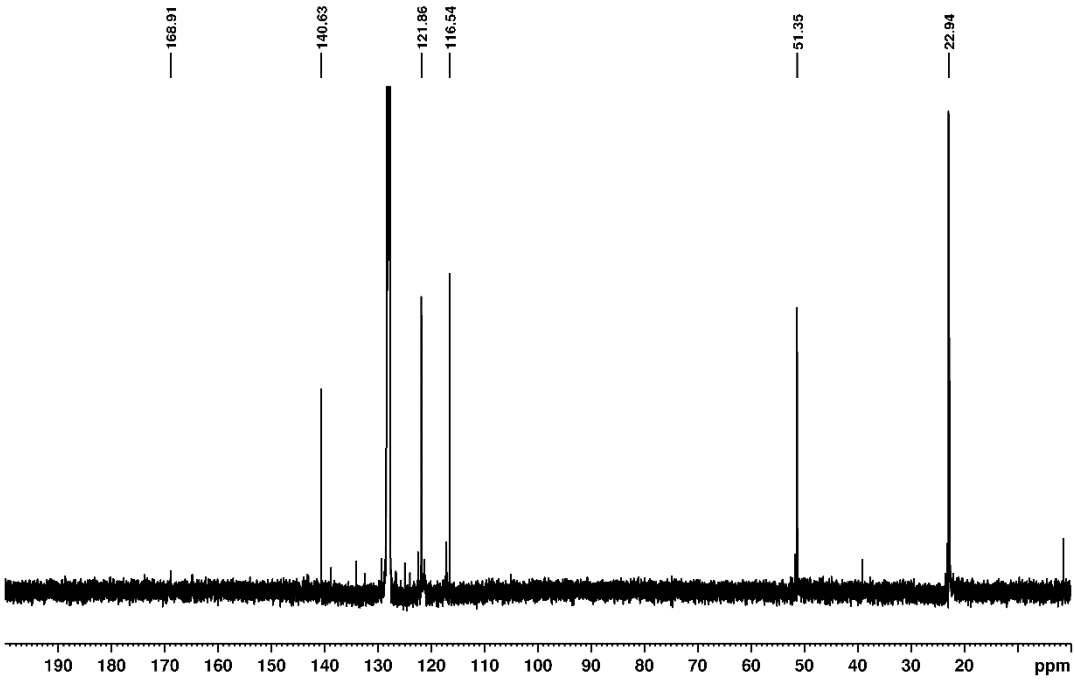

Figure S22. ^{13}C NMR spectrum (100.6 MHz, C_6D_6, 298 K) of (I*i*Pr)·GaH_2Ind **8**.

(IMe^{Me})·GaH_2Ind **9**:

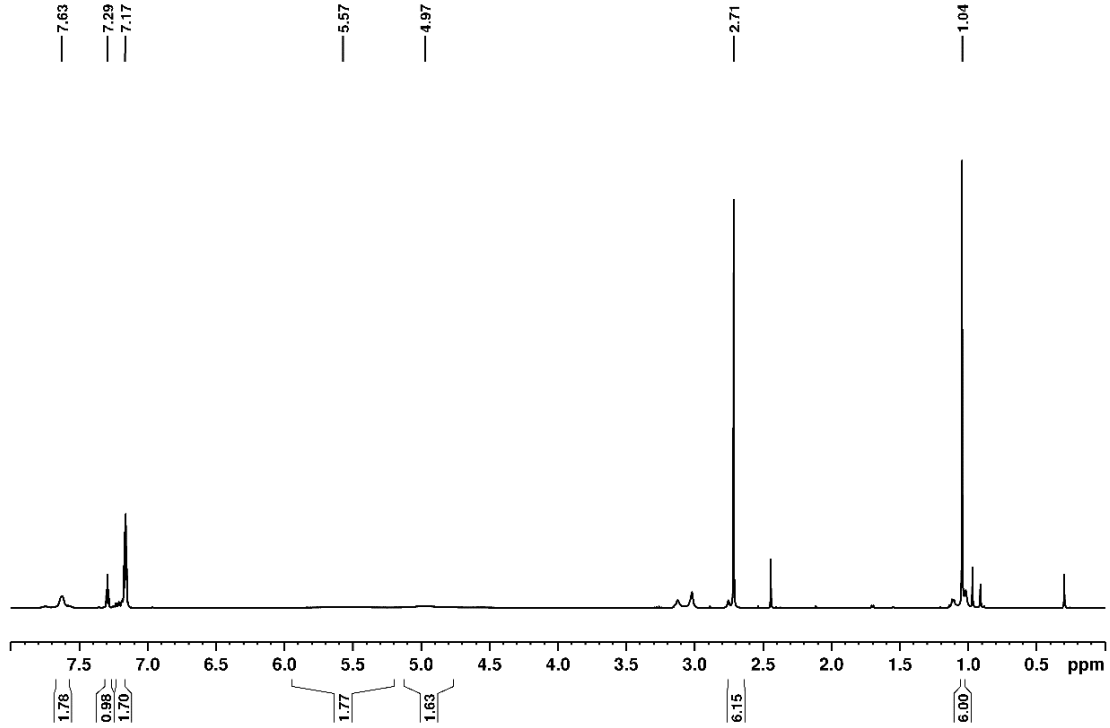

Figure S23. ^{1}H NMR spectrum (400.1 MHz, C_6D_6, 298 K) of (IMe^{Me})·GaH_2Ind **9** (unmarked signals belong to unknown impurities).

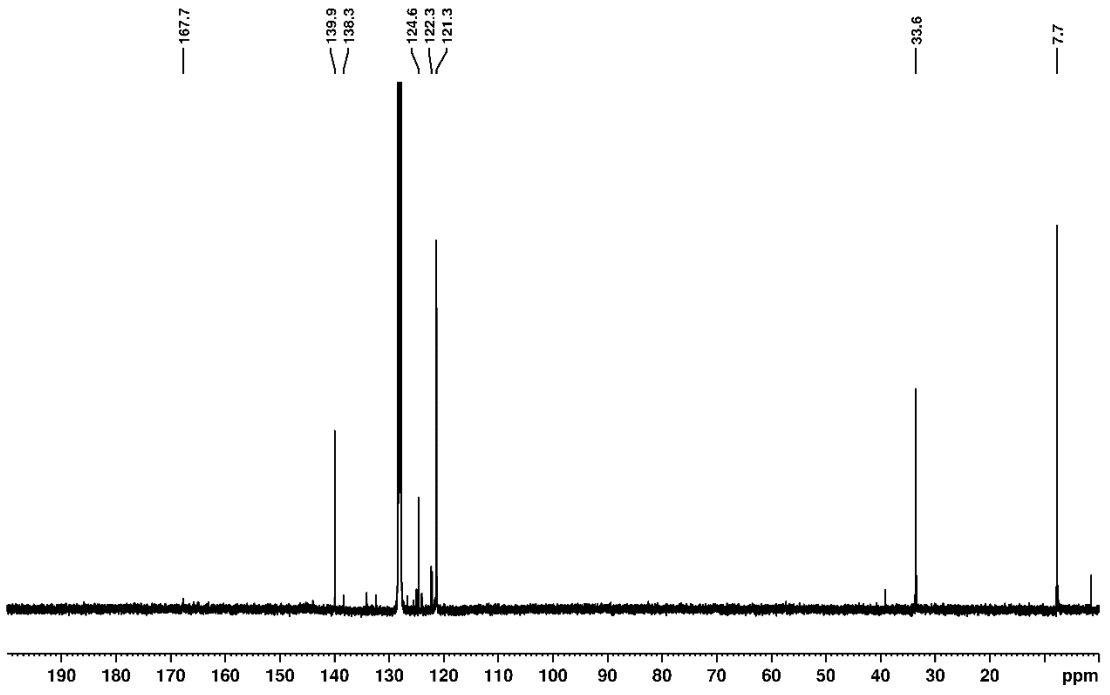

Figure S24. ^{13}C NMR spectrum (100.6 MHz, C_6D_6, 298 K) of (IMe^{Me})·GaH_2Ind **9**.

(I*i*Pr^{Me})·GaH$_2$Fl **10**:

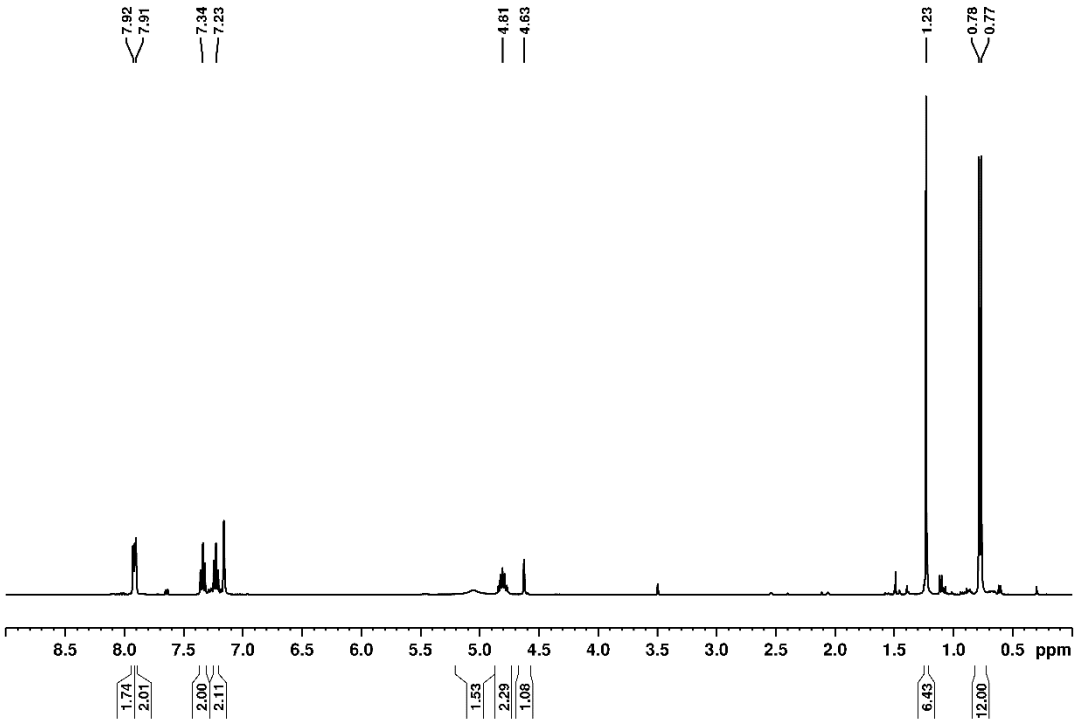

Figure S25. ^{1}H NMR spectrum (400.1 MHz, C_6D_6, 298 K) of (I*i*Pr^{Me})·GaH$_2$Fl **10**.

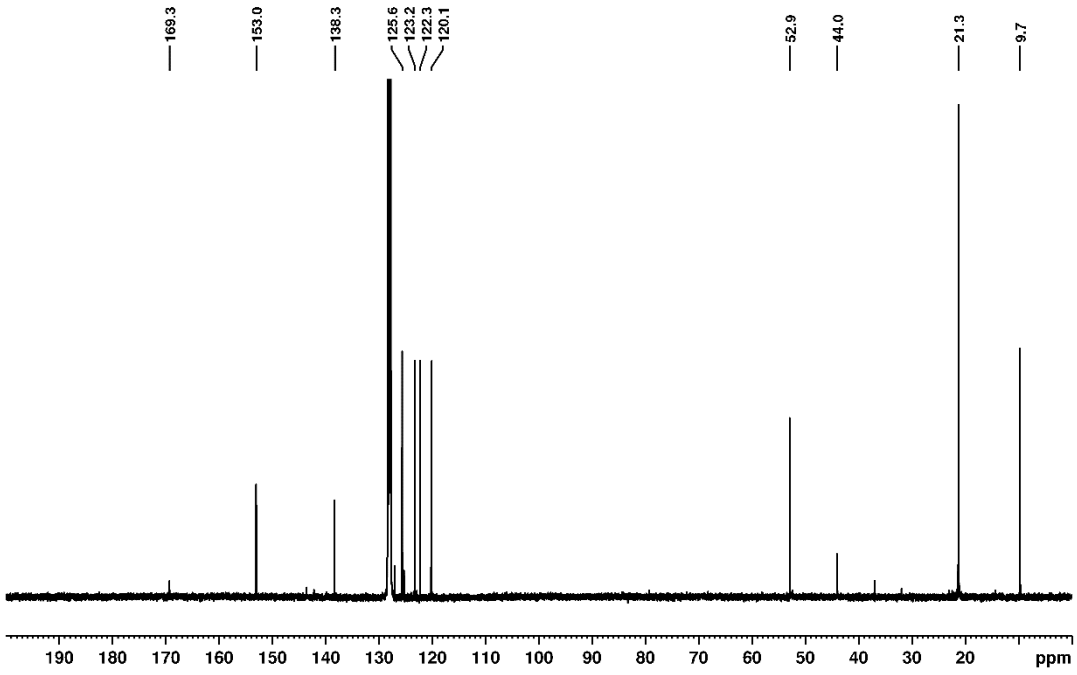

Figure S26. ^{13}C NMR spectrum (100.6 MHz, C_6D_6, 298 K) of (I*i*Pr^{Me})·GaH$_2$Fl **10**.

(I*i*Pr)·GaH_2Fl **11**:

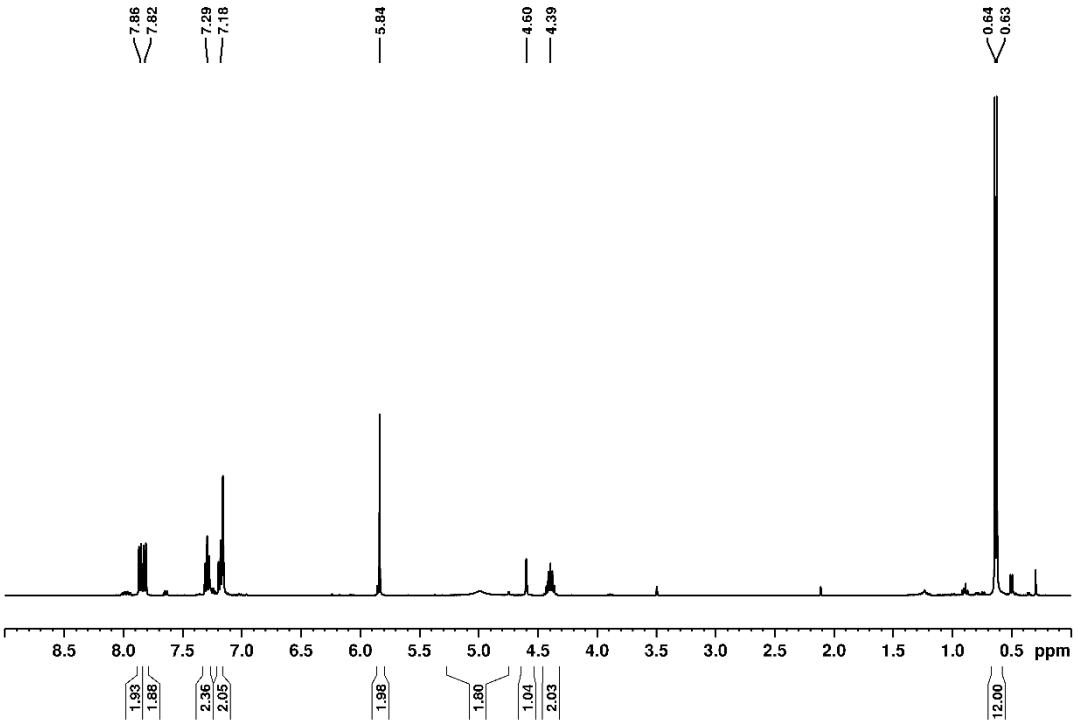

Figure S27. ^{1}H NMR spectrum (400.1 MHz, C_6D_6, 298 K) of (I*i*Pr)·GaH_2Fl **11**.

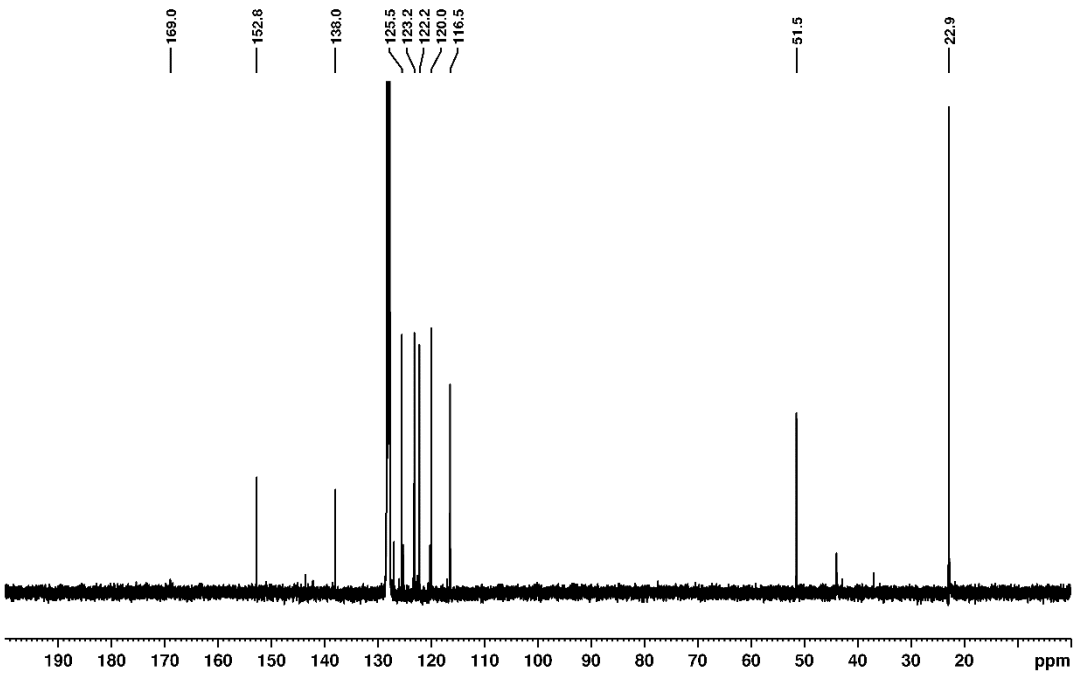

Figure S28. ^{13}C NMR spectrum (100.6 MHz, C_6D_6, 298 K) of (I*i*Pr)·GaH_2Fl **11**.

(IMe^{Me})·GaH_2Fl **12**:

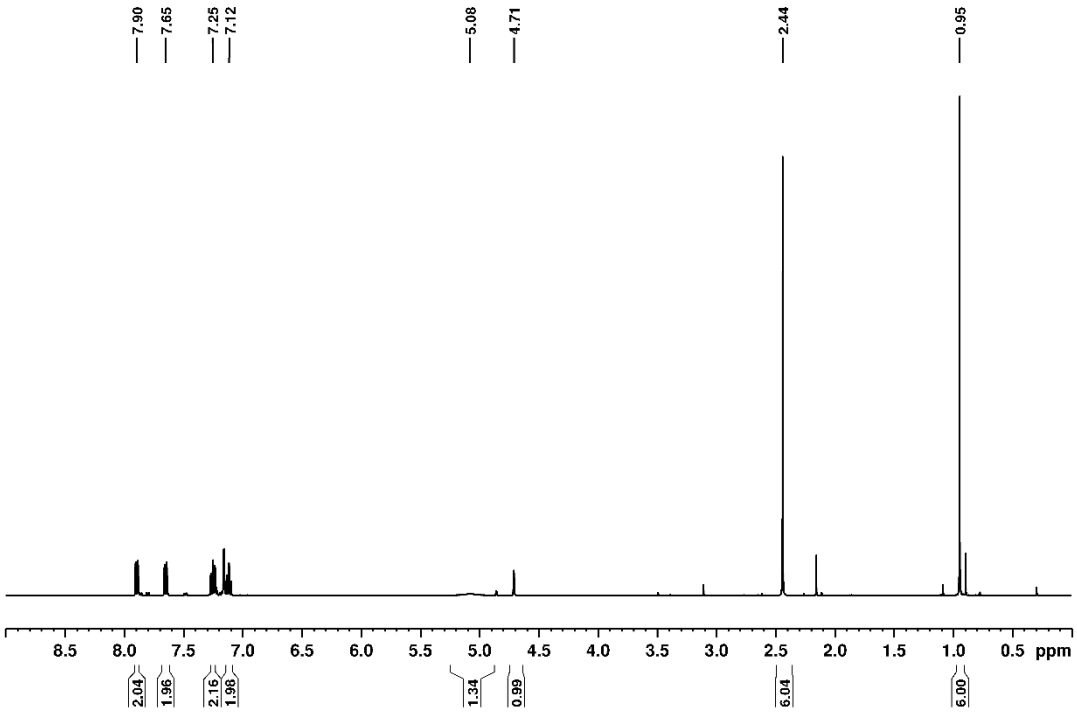

Figure S29. ^{1}H NMR spectrum (400.1 MHz, C_6D_6, 298 K) of (IMe^{Me})·GaH_2Fl **12**.

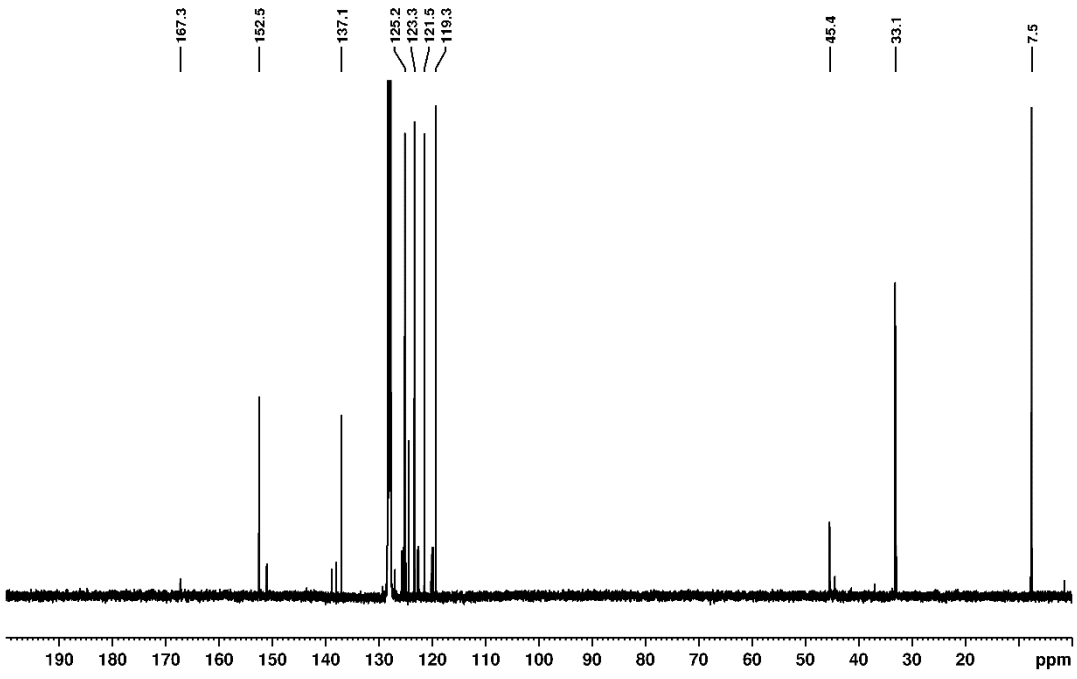

Figure S30. ^{13}C NMR spectrum (100.6 MHz, C_6D_6, 298 K) of (IMe^{Me})·GaH_2Fl **12**.

(I*i*Pr^{Me})·AlHInd$_2$ **13**:

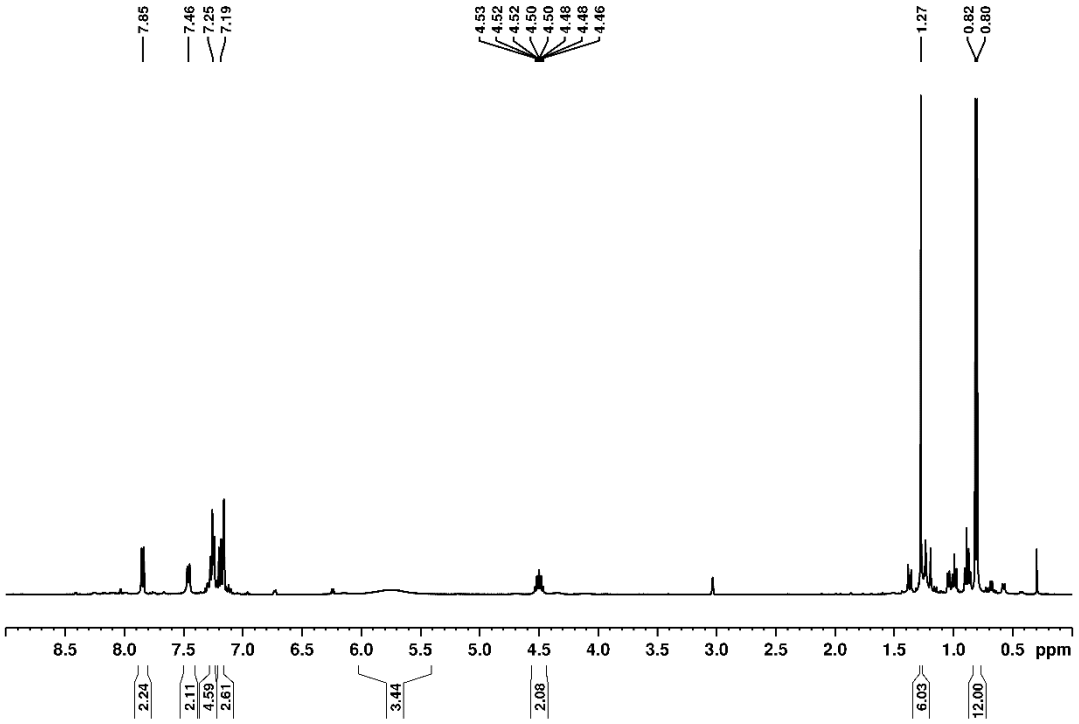

Figure S31. ^{1}H NMR spectrum (400.1 MHz, C_6D_6, 298 K) of (I*i*Pr^{Me})·AlHInd$_2$ **13** (unmarked signals belong to unknown impurities).

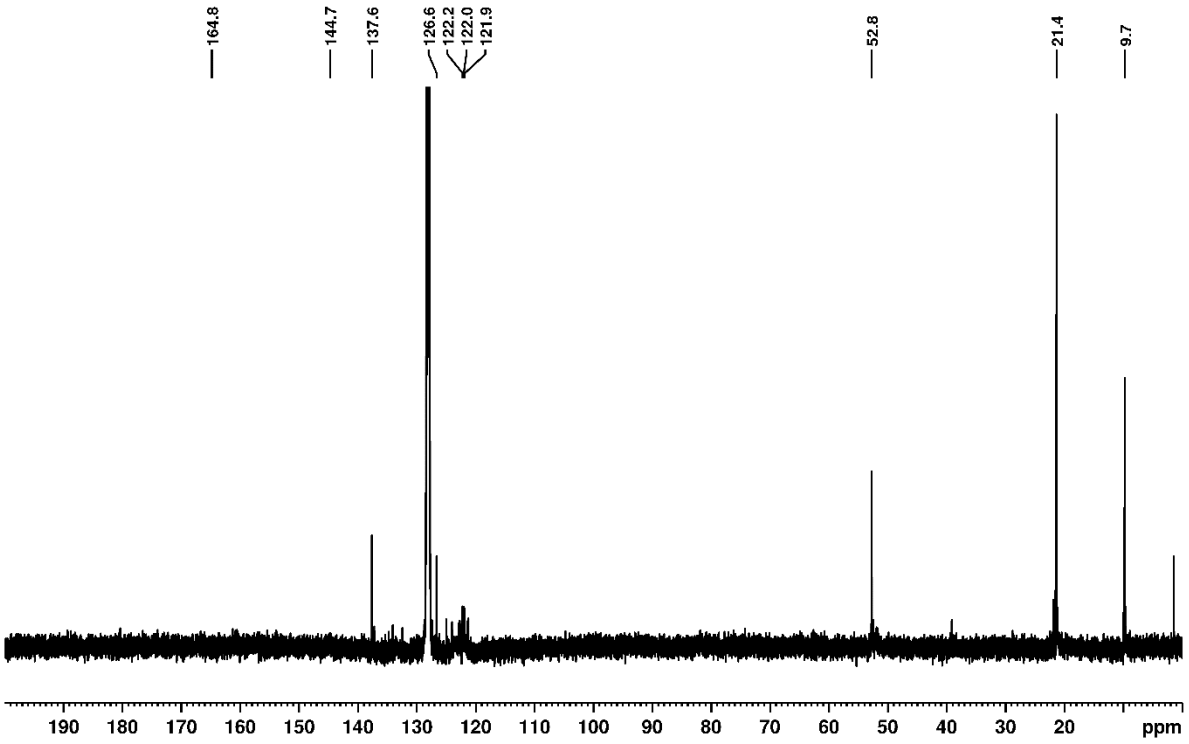

Figure S32. ^{13}C NMR spectrum (100.6 MHz, C_6D_6, 298 K) of (I*i*Pr^{Me})·AlHInd$_2$ **13**.

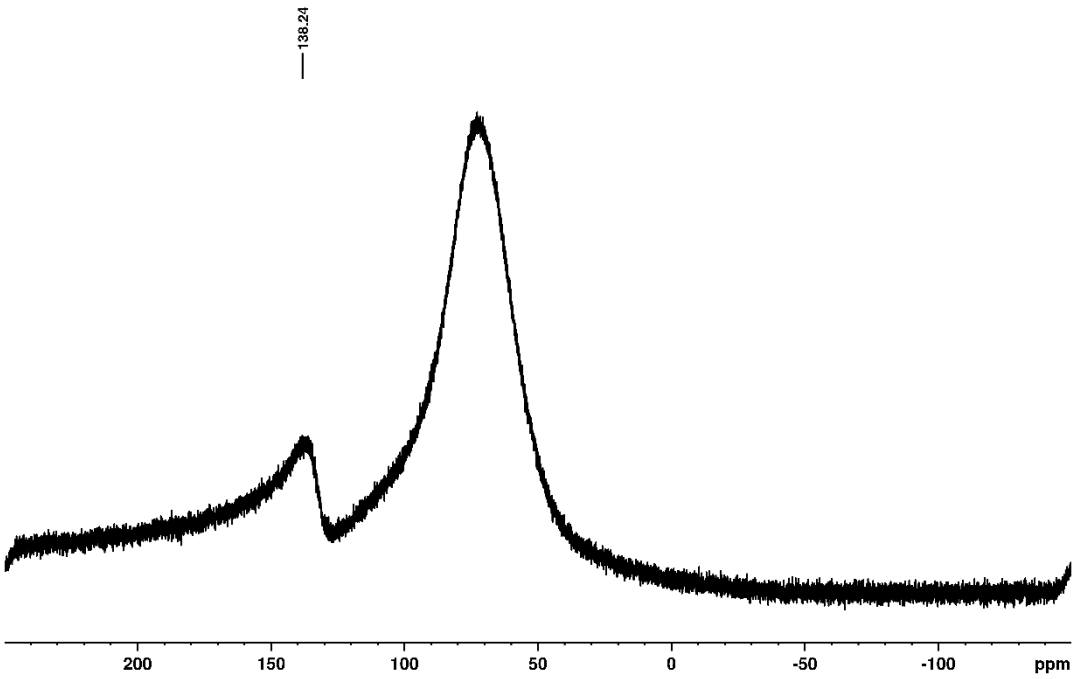

Figure S33. ^{27}Al NMR spectrum (104.3 MHz, C_6D_6, 298 K) of (I*i*Pr^{Me})·AlHInd$_2$ **13**.

(I*i*Pr)·AlHInd$_2$ **14**:

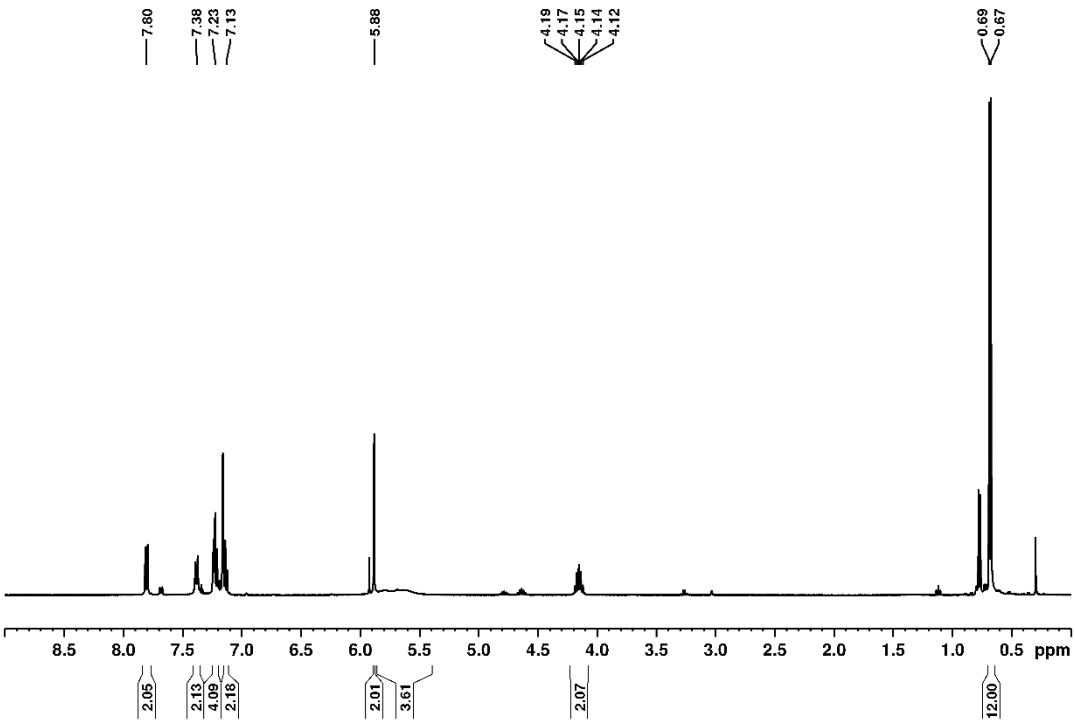

Figure S34. ^{1}H NMR spectrum (400.1 MHz, C_6D_6, 298 K) of (I*i*Pr)·AlHInd$_2$ **14** (unmarked signals belong to unknown impurities).

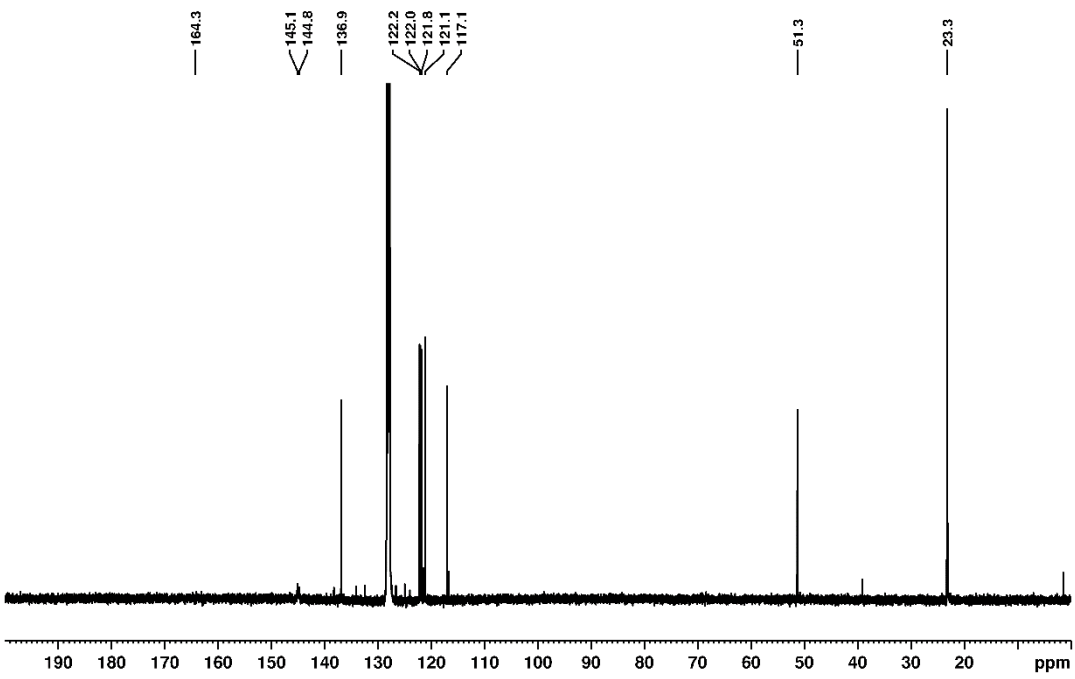

Figure S35. ^{13}C NMR spectrum (100.6 MHz, C_6D_6, 298 K) of (I*i*Pr)·AlHInd$_2$ **14.**

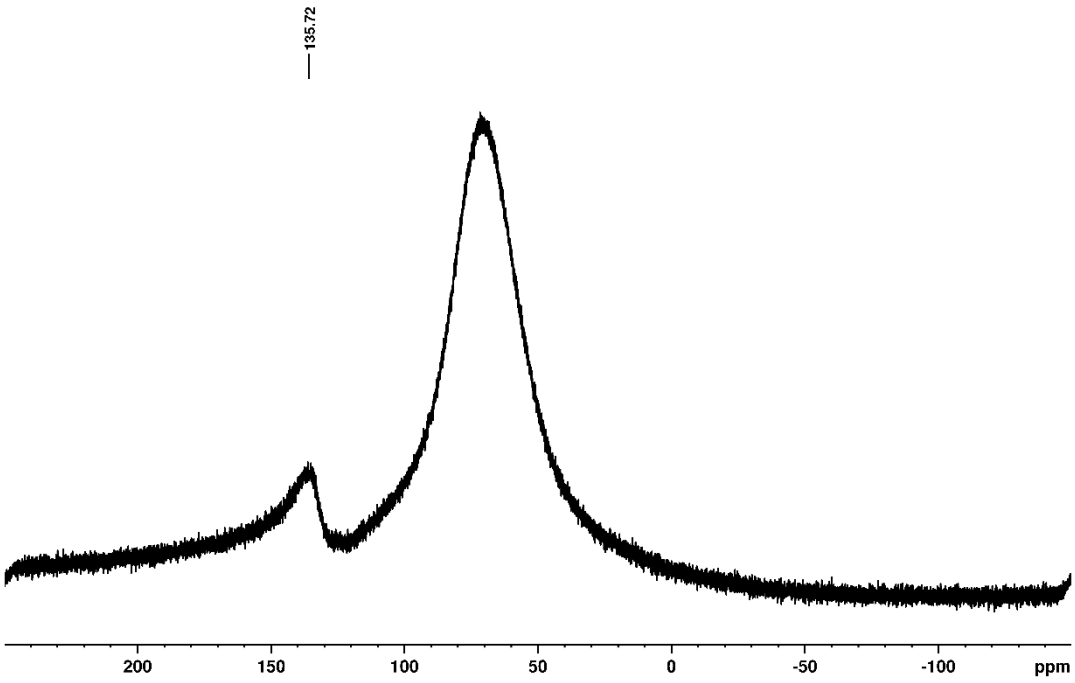

Figure S36. ^{27}Al NMR spectrum (104.3 MHz, C_6D_6, 298 K) of (I*i*Pr)·AlHInd$_2$ **14**.

(IMe^{Me})·$AlHInd_2$ **15**:

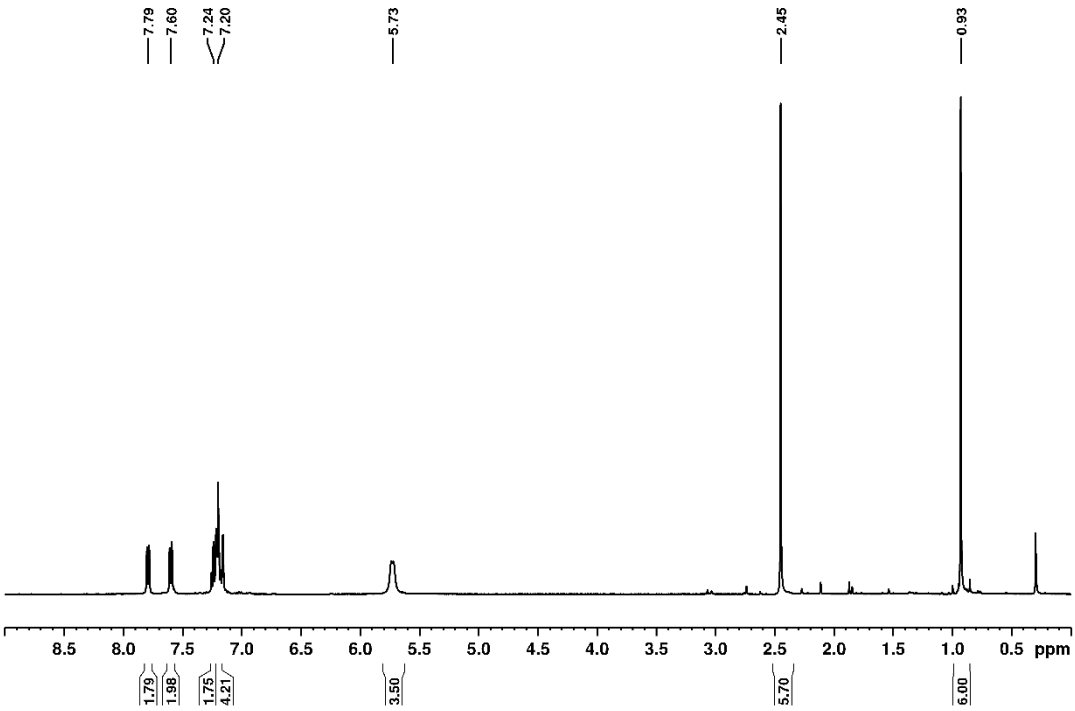

Figure S37. ^{1}H NMR spectrum (400.1 MHz, C_6D_6, 298 K) of (IMe^{Me})·$AlHInd_2$ **15.**

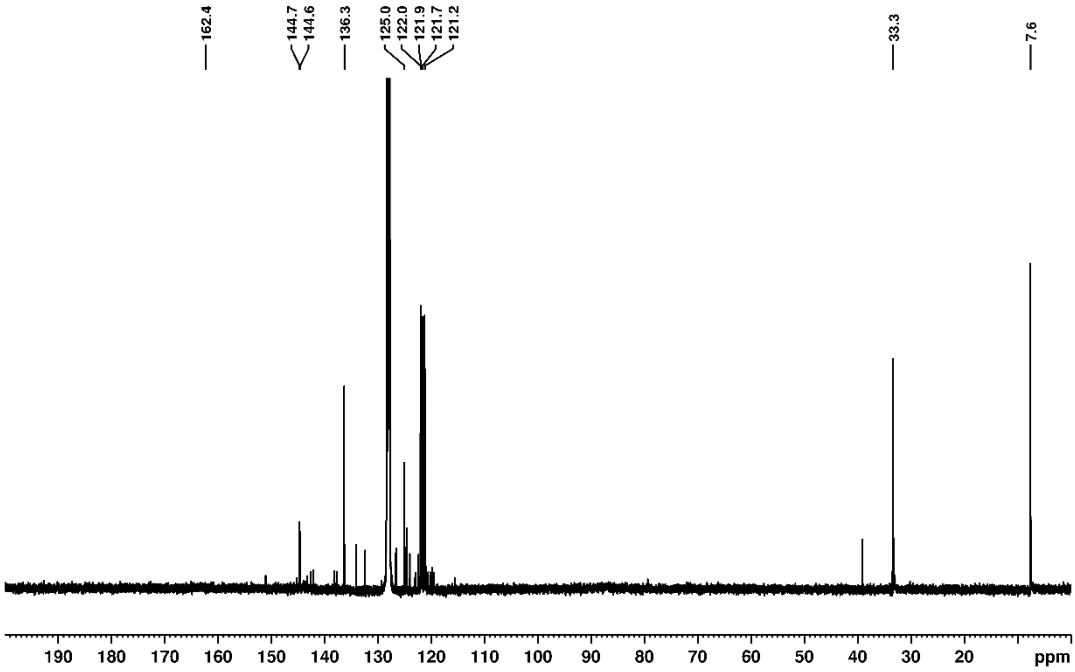

Figure S38. ^{13}C NMR spectrum (100.6 MHz, C_6D_6, 298 K) of (IMe^{Me})·$AlHInd_2$ **15.**

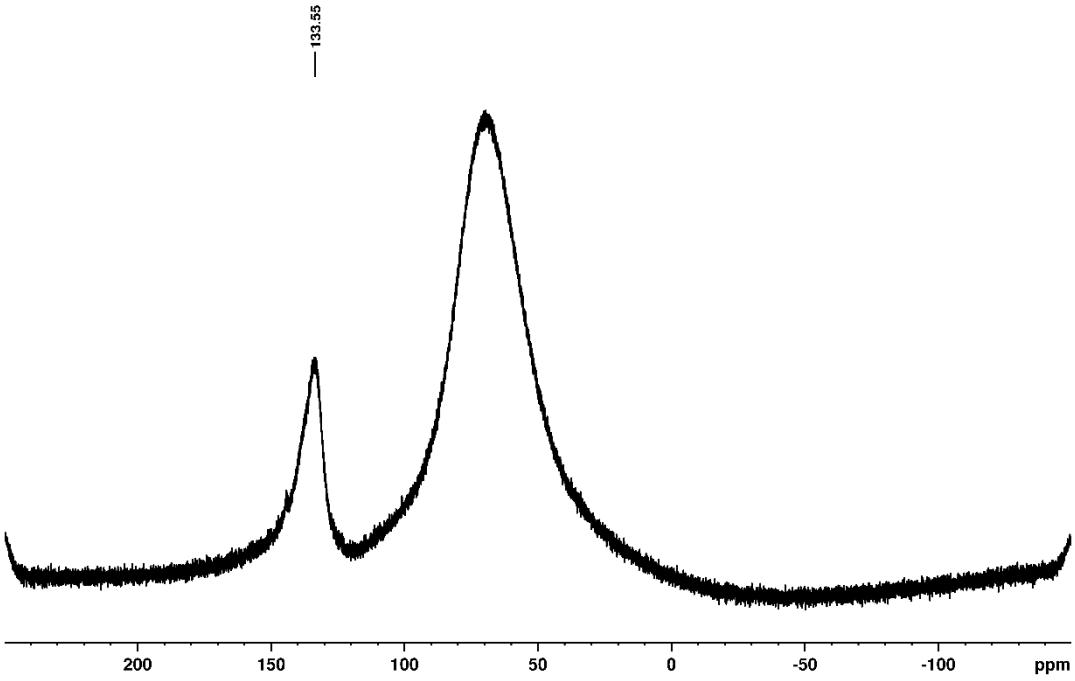

Figure S39. ^{27}Al NMR spectrum (104.3 MHz, C_6D_6, 298 K) of (IMe^{Me})·AlHInd$_2$ **15**.

(I*i*Pr^{Me})·AlHFl$_2$ **16**:

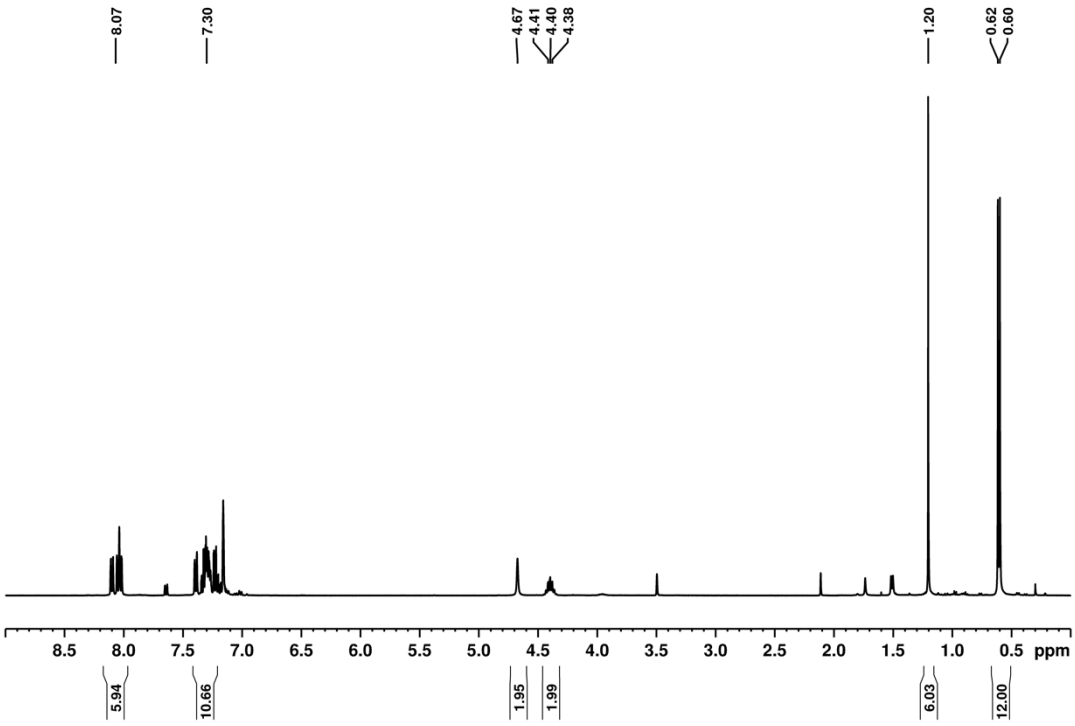

Figure S40. ^{1}H NMR spectrum (400.1 MHz, C_6D_6, 298 K) of (I*i*Pr^{Me})·AlHFl$_2$ **16**.

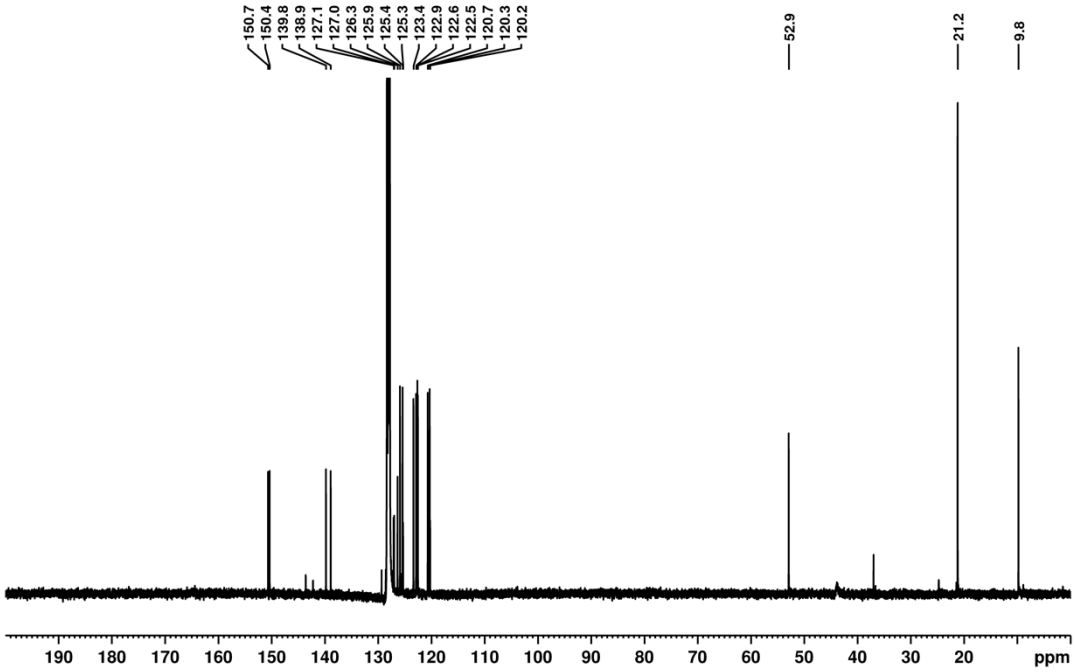

Figure S41. ^{13}C NMR spectrum (100.6 MHz, C_6D_6, 298 K) of (I*i*Pr^{Me})·AlHFl$_2$ **16.**

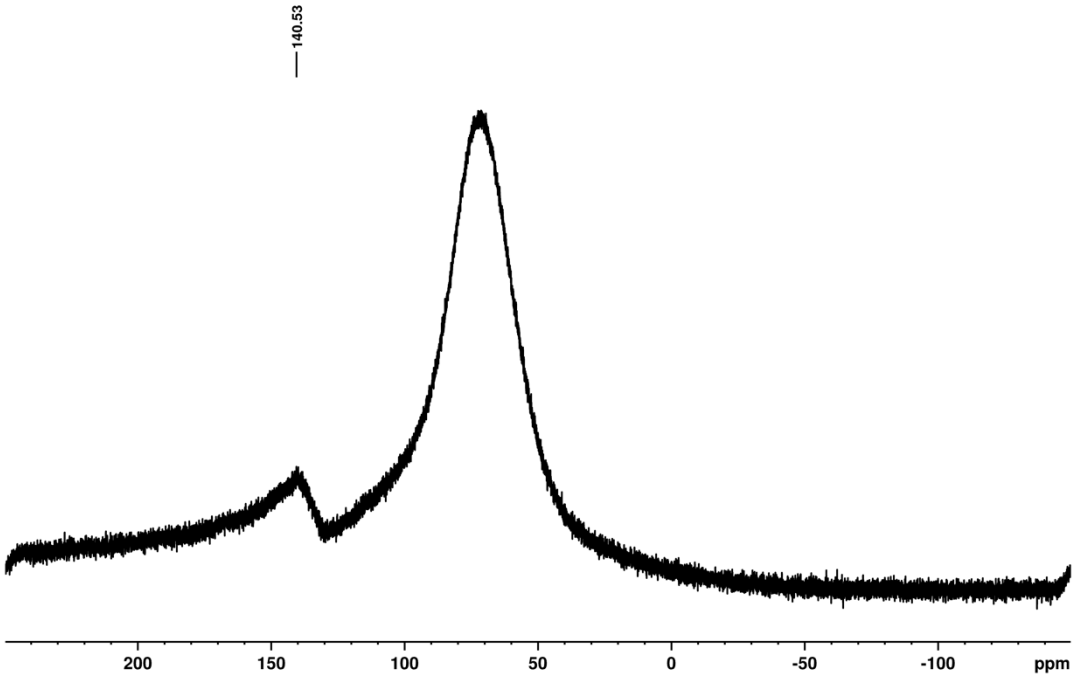

Figure S42. ^{27}Al NMR spectrum (104.3 MHz, C_6D_6, 298 K) of (I*i*Pr^{Me})·AlHFl$_2$ **16**.

(I*i*Pr)·AlHFl$_2$ **17**:

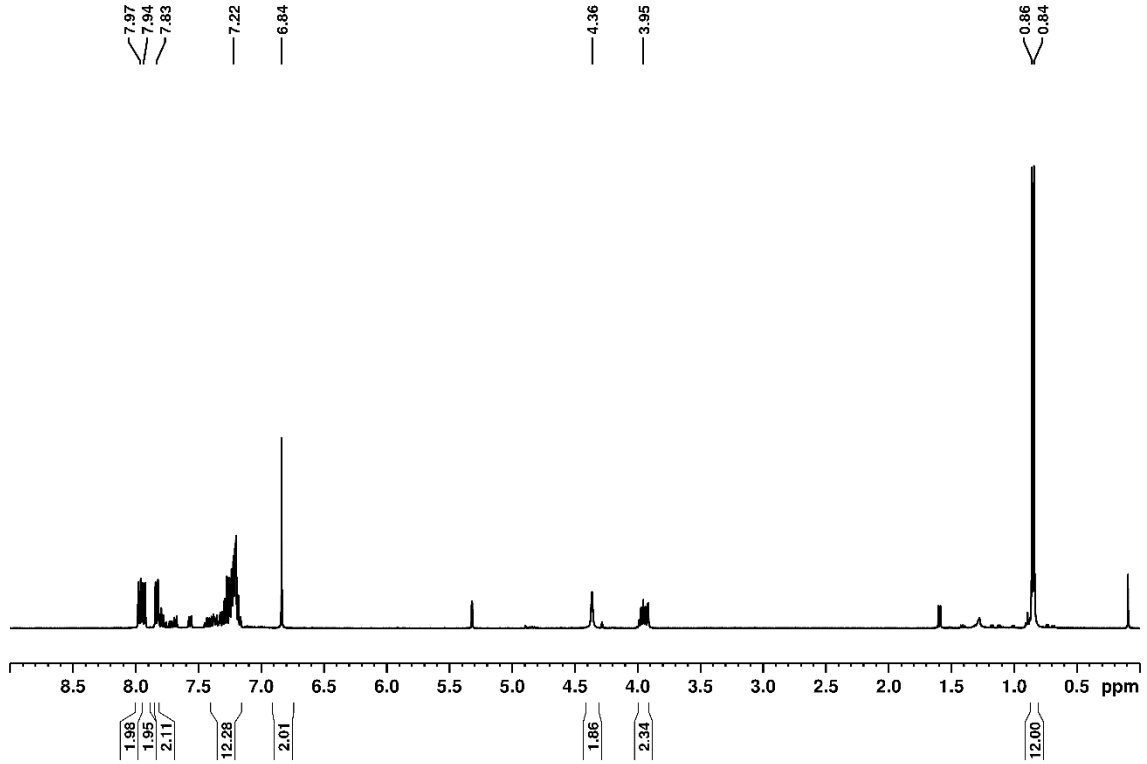

Figure S43. ^{1}H NMR spectrum (400.1 MHz, CD_2Cl_2, 298 K) of (I*i*Pr)·AlHFl$_2$ **17** (unmarked signals belong to unknown impurities due to minor decomposition in CD_2Cl_2)**.**

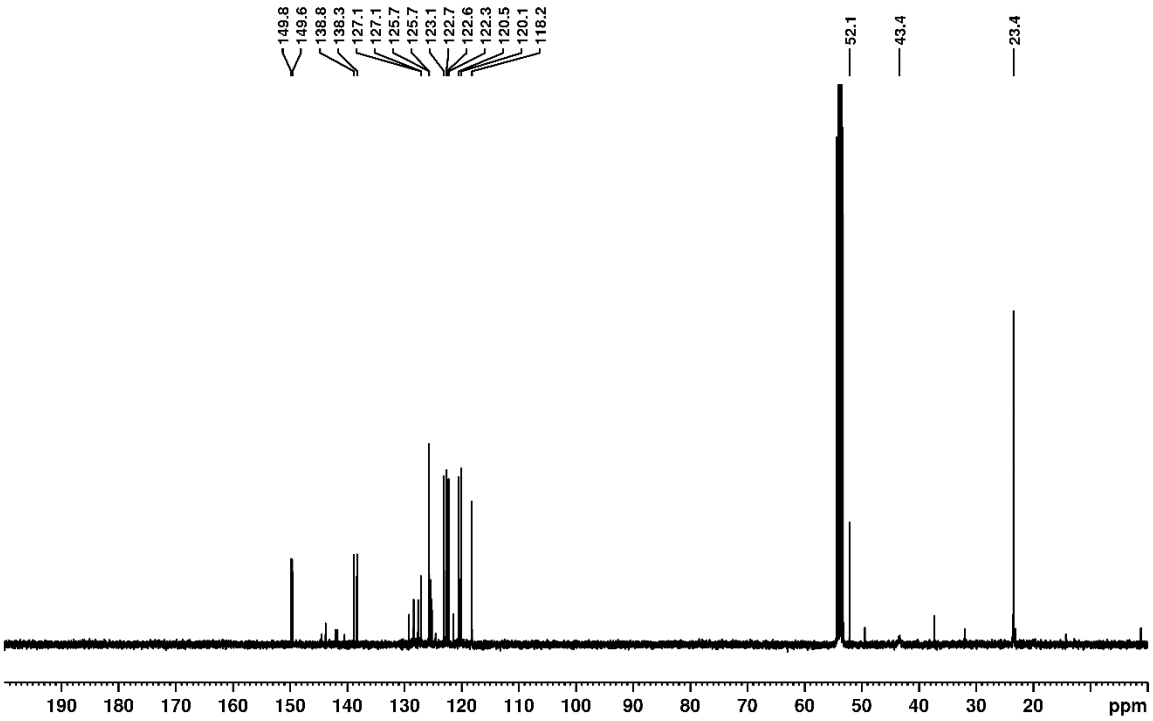

Figure S44. ^{13}C NMR spectrum (100.6 MHz, CD_2Cl_2, 298 K) of (I*i*Pr)·AlHFl$_2$ **17** (unmarked signals belong to unknown impurities due to minor decomposition in CD_2Cl_2).

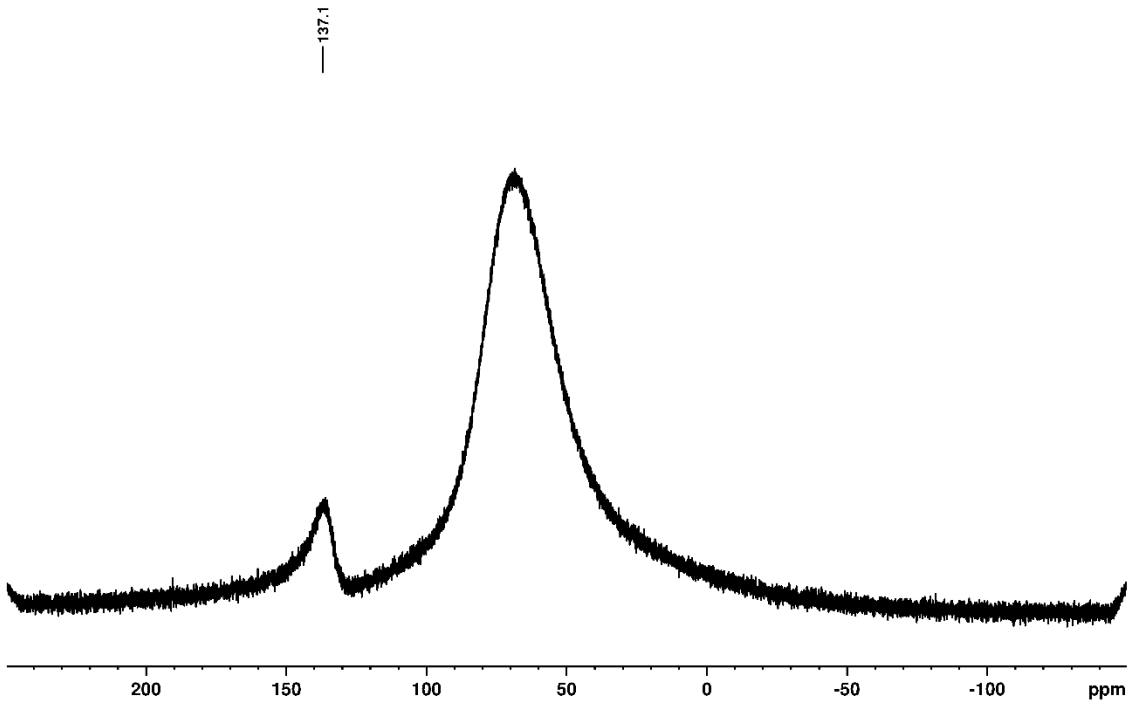

Figure S45. ^{27}Al NMR spectrum (104.3 MHz, CD_2Cl_2, 298 K) of (I*i*Pr)·$AlHFl_2$ **17**.

(IMe^{Me})·$AlHFl_2$ **18**:

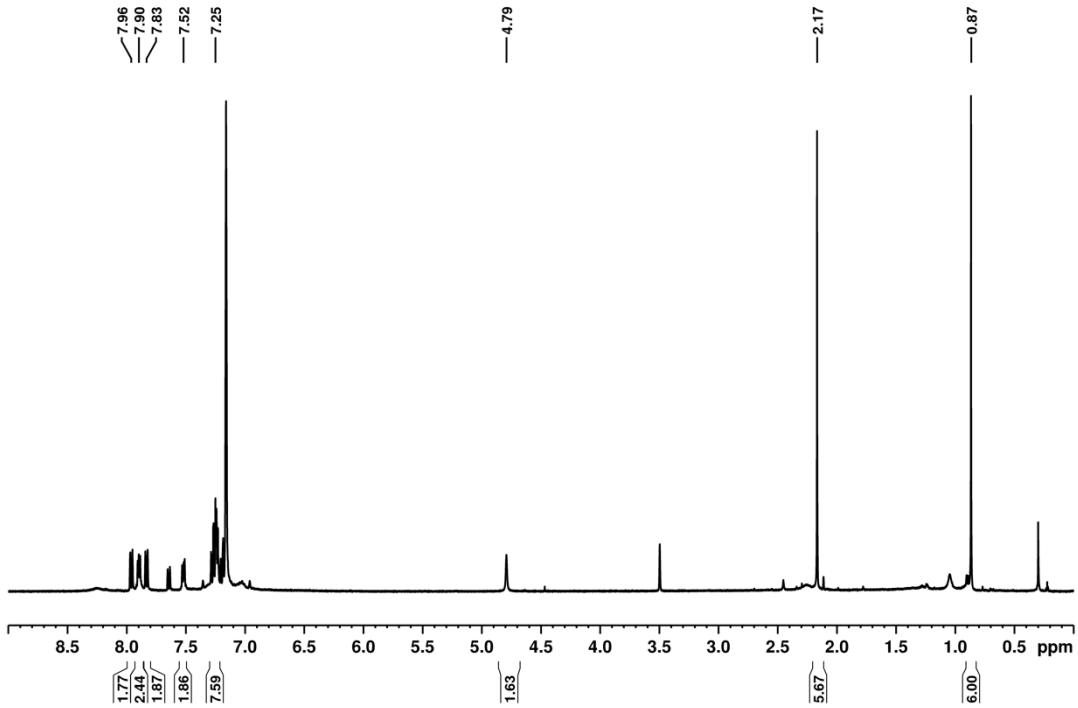

Figure S46. ^{1}H NMR spectrum (400.1 MHz, C_6D_6, 298 K) of (IMe^{Me})·$AlHFl_2$ **18.**

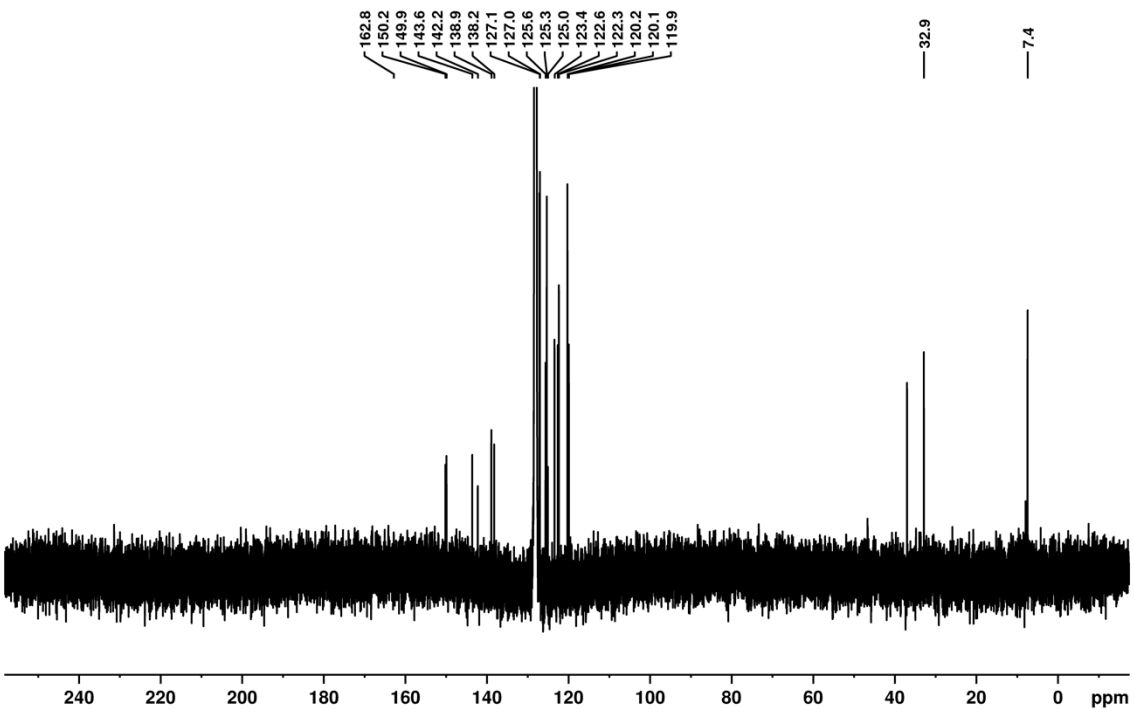

Figure S47. ^{13}C NMR spectrum (100.6 MHz, C_6D_6, 298 K) of (IMe^{Me})·$AlHFl_2$ **18.**

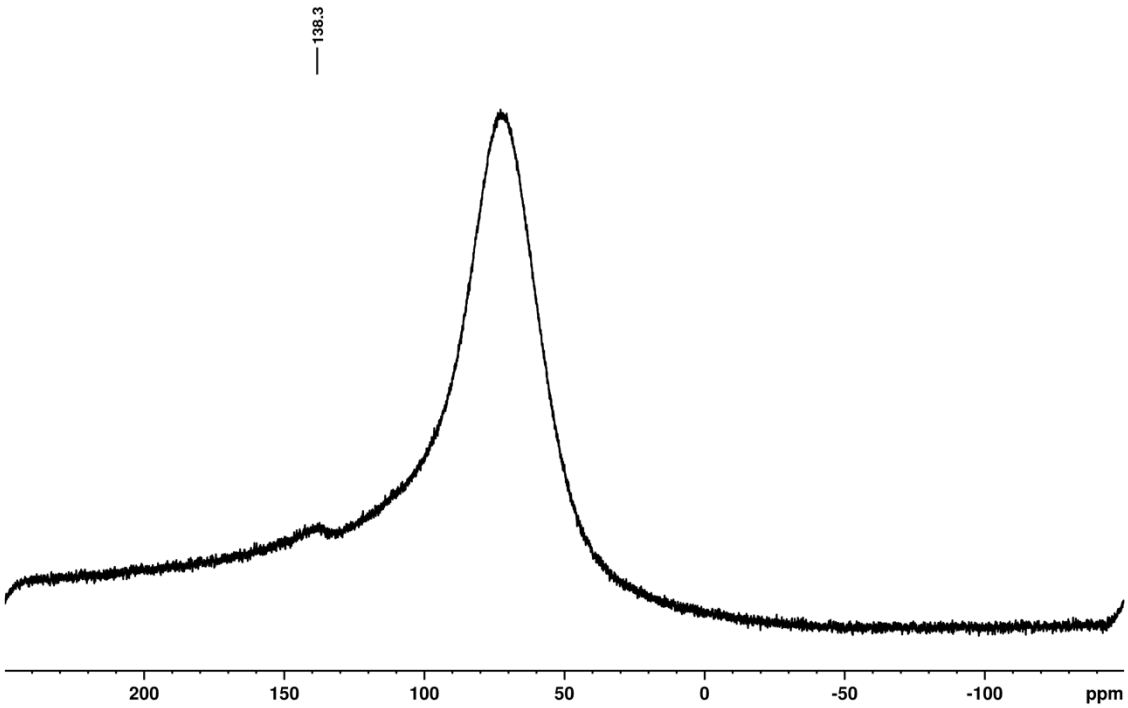

Figure S48. ^{27}Al NMR spectrum (104.3 MHz, C_6D_6, 298 K) of (IMe^{Me})·$AlHFl_2$ **18**.

((I*i*Pr^{Me})·AlH$_2$)$_2$-μ-Fl **19**:

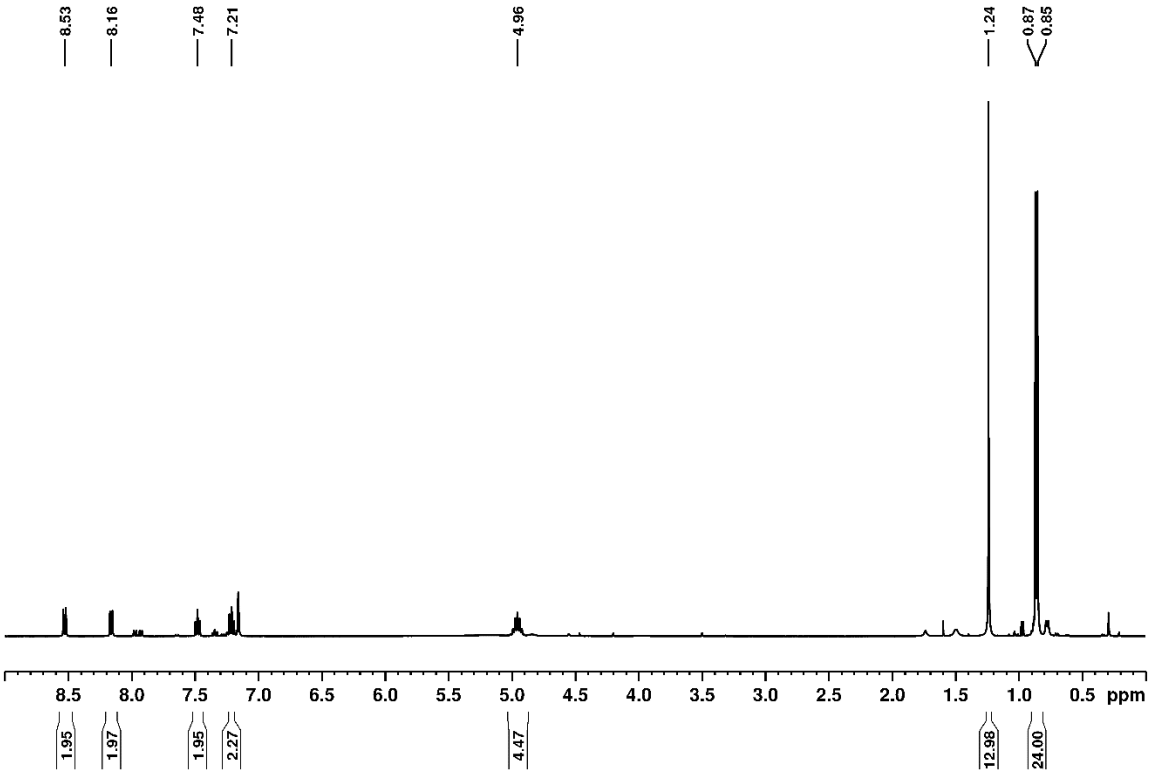

Figure S49. ^{1}H NMR spectrum (400.1 MHz, C_6D_6, 298 K) of {(I*i*Pr^{Me})·AlH$_2$}$_2$-μ-Fl **19.**

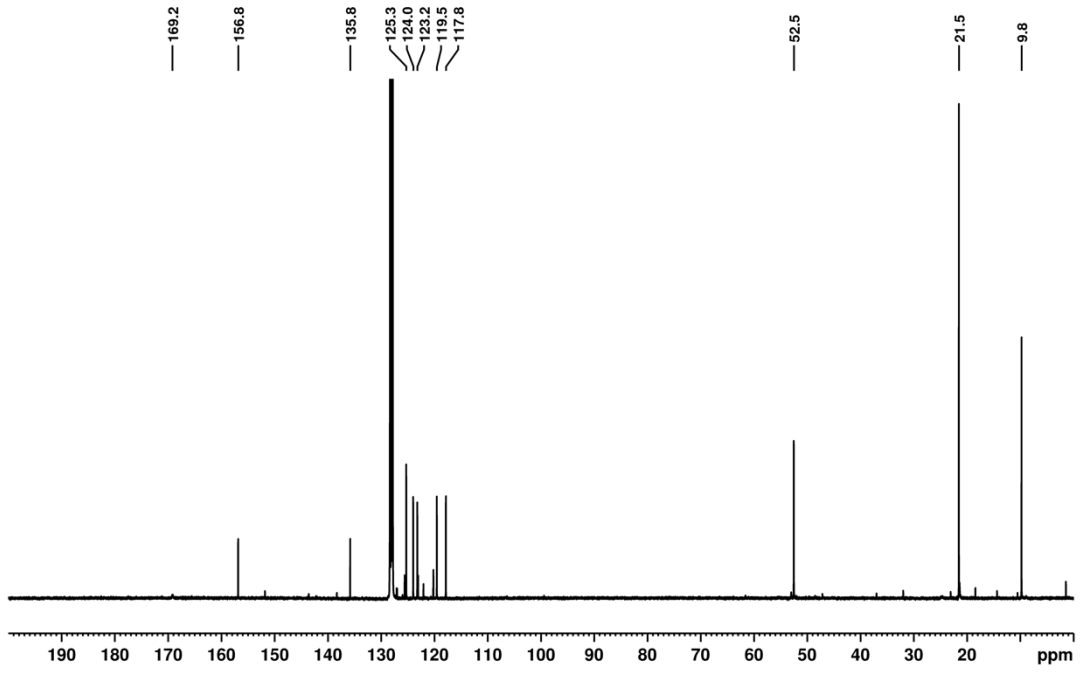

Figure S50. ^{13}C NMR spectrum (100.6 MHz, C_6D_6, 298 K) of {(I*i*Pr^{Me})·AlH$_2$}$_2$-μ-Fl **19.**

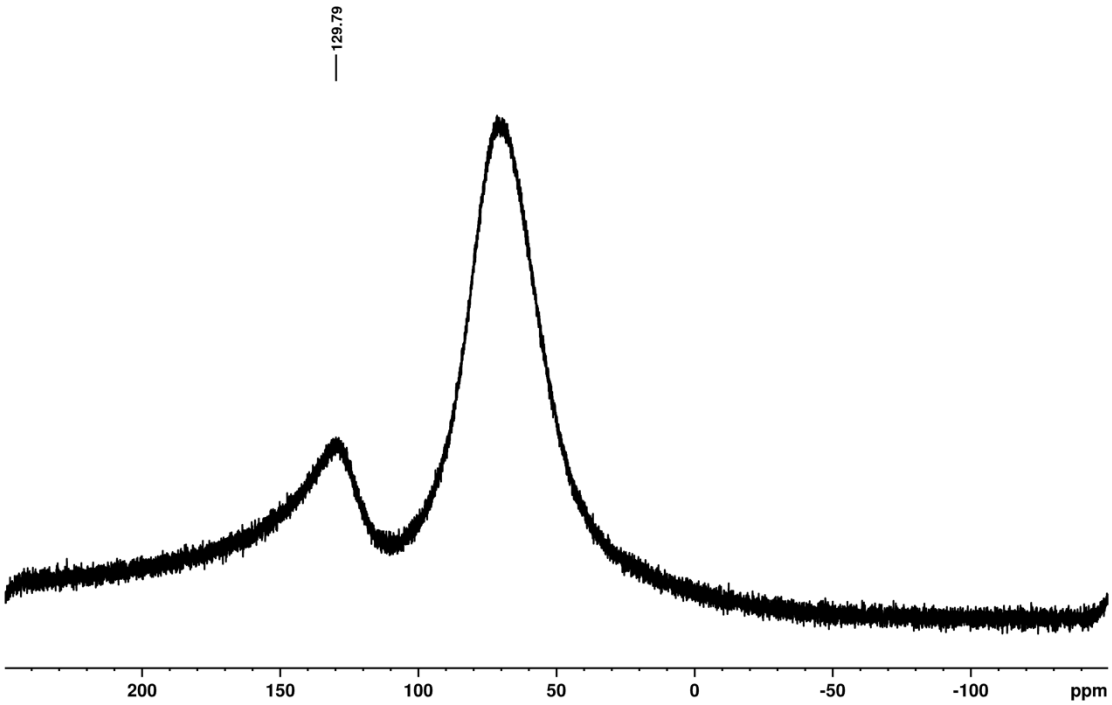

Figure S51. ^{27}Al NMR spectrum (104.3 MHz, C_6D_6, 298 K) of {(I*i*Pr^{Me})·AlH_2}$_2$-μ-Fl **19**.

((I*i*Pr)·AlH_2)$_2$-μ-Fl **20**:

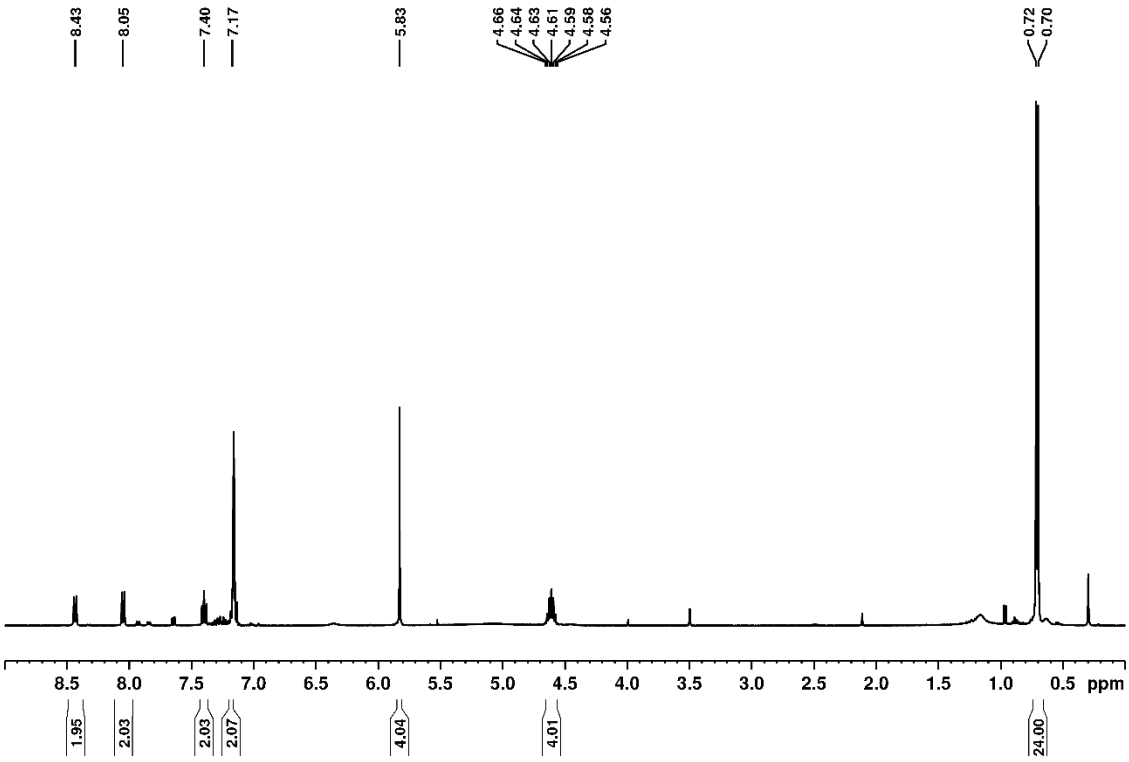

Figure S52. ^{1}H NMR spectrum (400.1 MHz, C_6D_6, 298 K) of {(I*i*Pr)·AlH_2}$_2$-μ-Fl **20.**

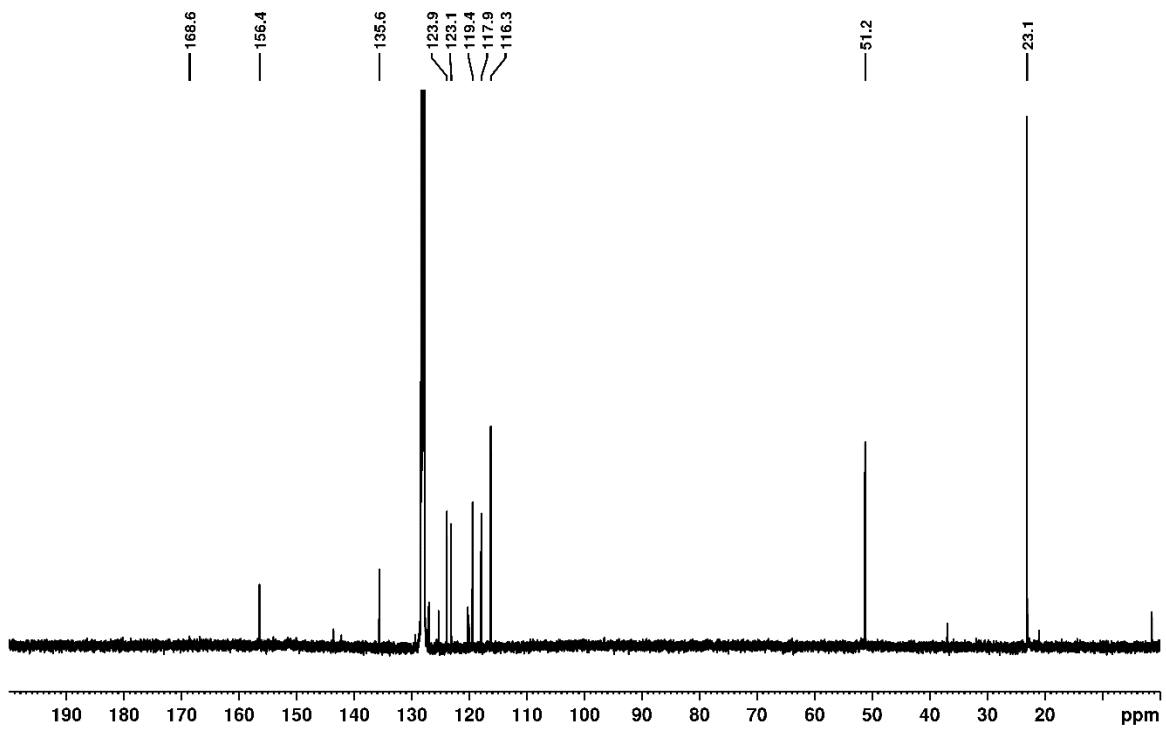

Figure S53. ^{13}C NMR spectrum (100.6 MHz, C_6D_6, 298 K) of {(I*i*Pr)·AlH_2}$_2$-μ-Fl **20.**

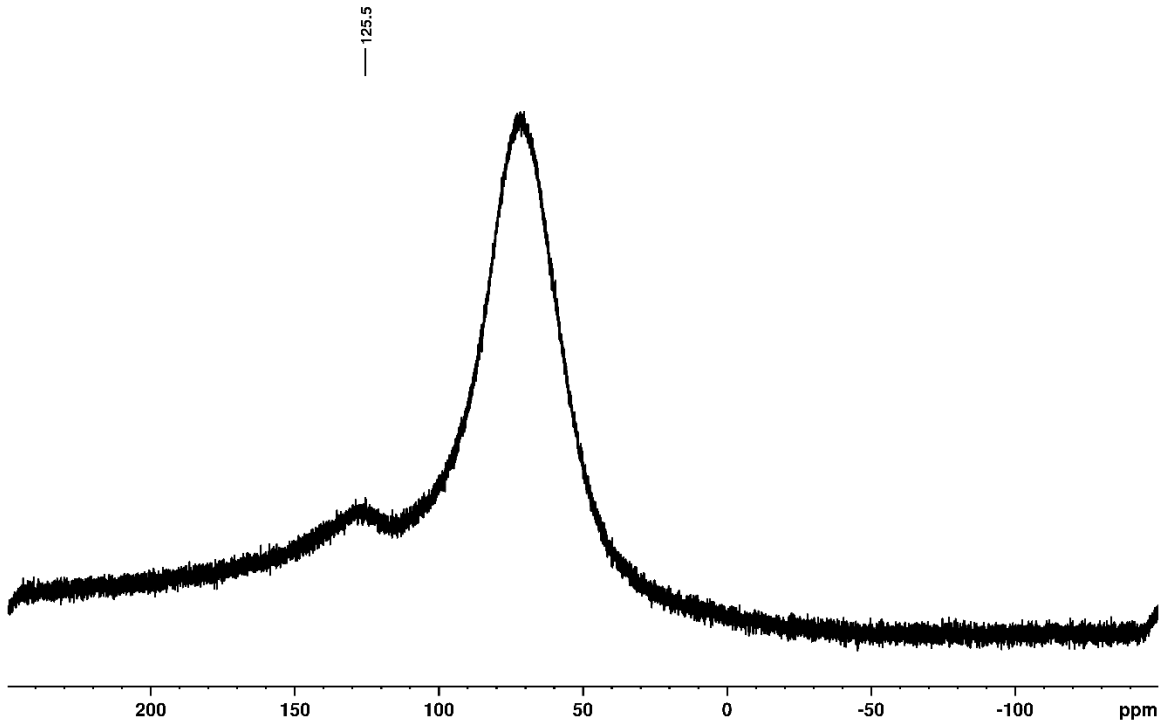

Figure S54. ^{27}Al NMR spectrum (104.3 MHz, C_6D_6, 298 K) of {(I*i*Pr)·AlH_2}$_2$-μ-Fl **20**.

((I*i*Pr^{Me})·AlH-μ-Fl)$_2$ **21**:

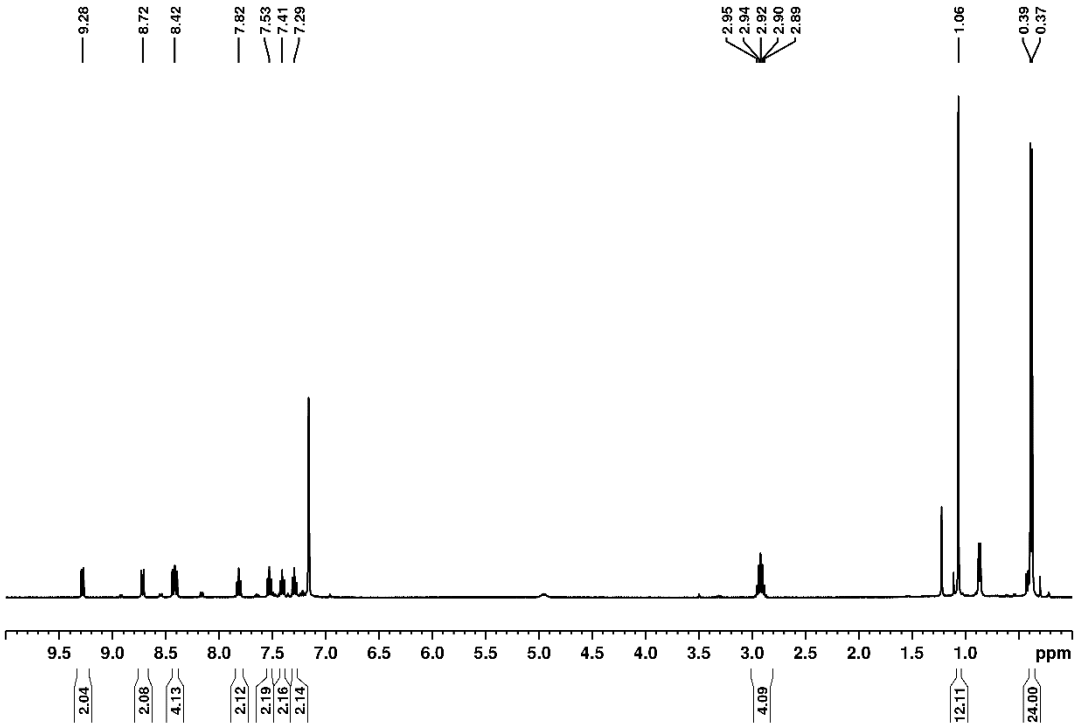

Figure S55. ^{1}H NMR spectrum (400.1 MHz, C_6D_6, 298 K) of {(I*i*Pr^{Me})·AlH-μ-Fl}$_2$ **21.**

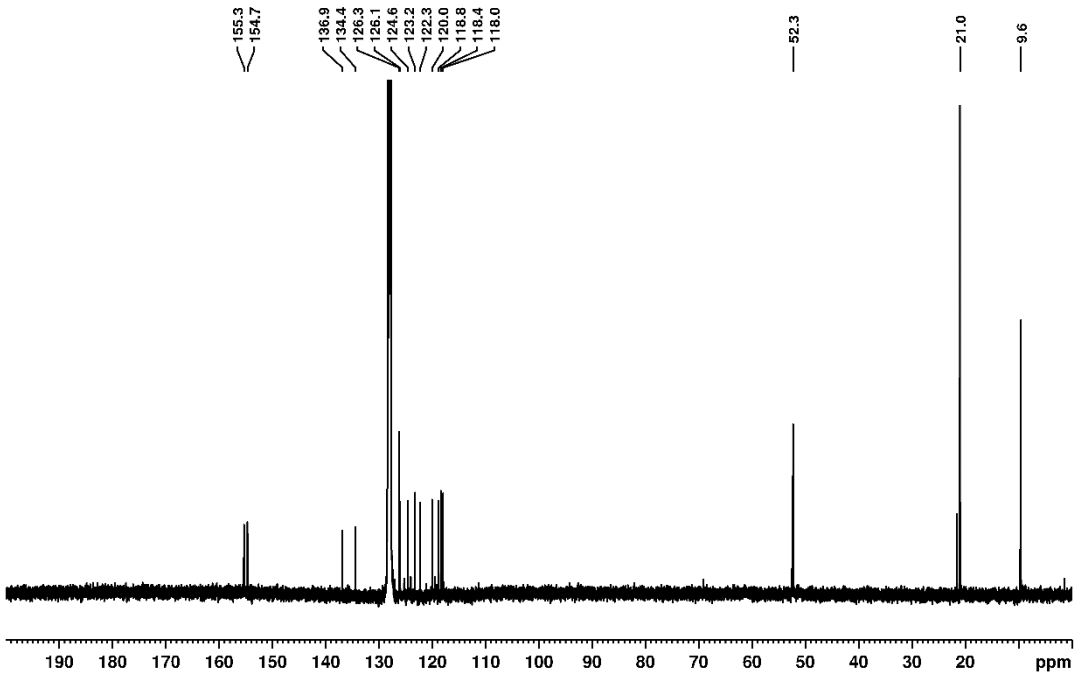

Figure S56. ^{13}C NMR spectrum (100.6 MHz, C_6D_6, 298 K) of {(I*i*Pr^{Me})·AlH-μ-Fl}$_2$ **21.**

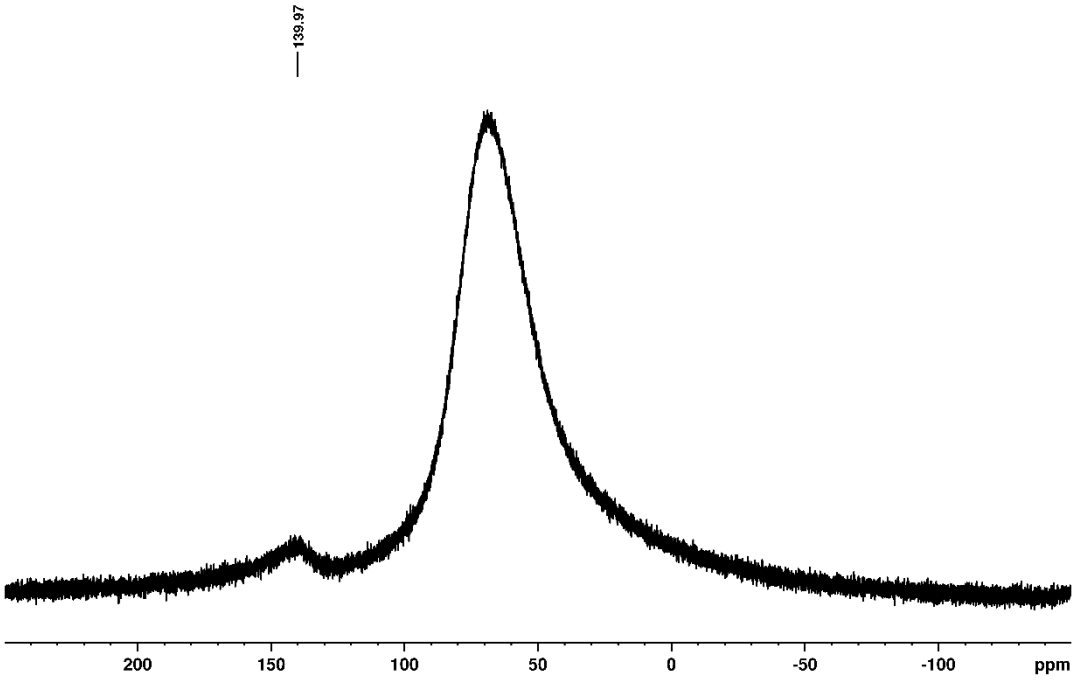

Figure S57. ^{27}Al NMR spectrum (104.3 MHz, C_6D_6, 298 K) of {(I*i*Pr^{Me})·AlH-μ-Fl}$_2$ **21**.

((I*i*Pr^{Me})·AlH-μ-Ind)$_2$ **22**:

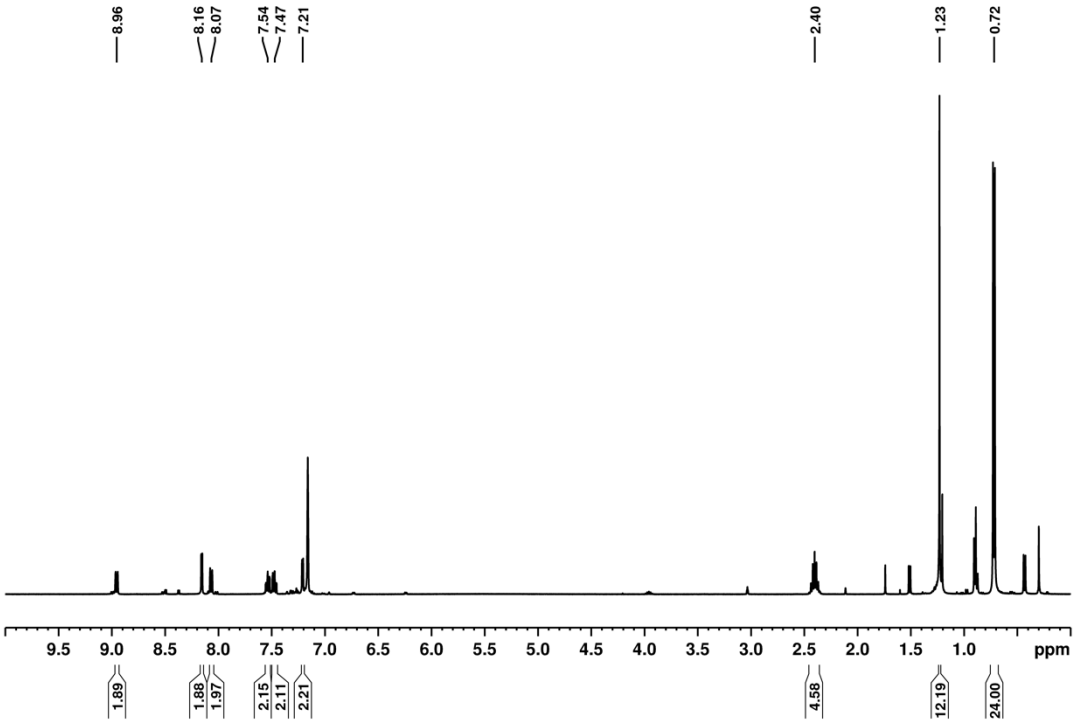

Figure S58. ^{1}H NMR spectrum (400.1 MHz, C_6D_6, 298 K) of {(I*i*Pr^{Me})·AlH-μ-Ind}$_2$ **22.**

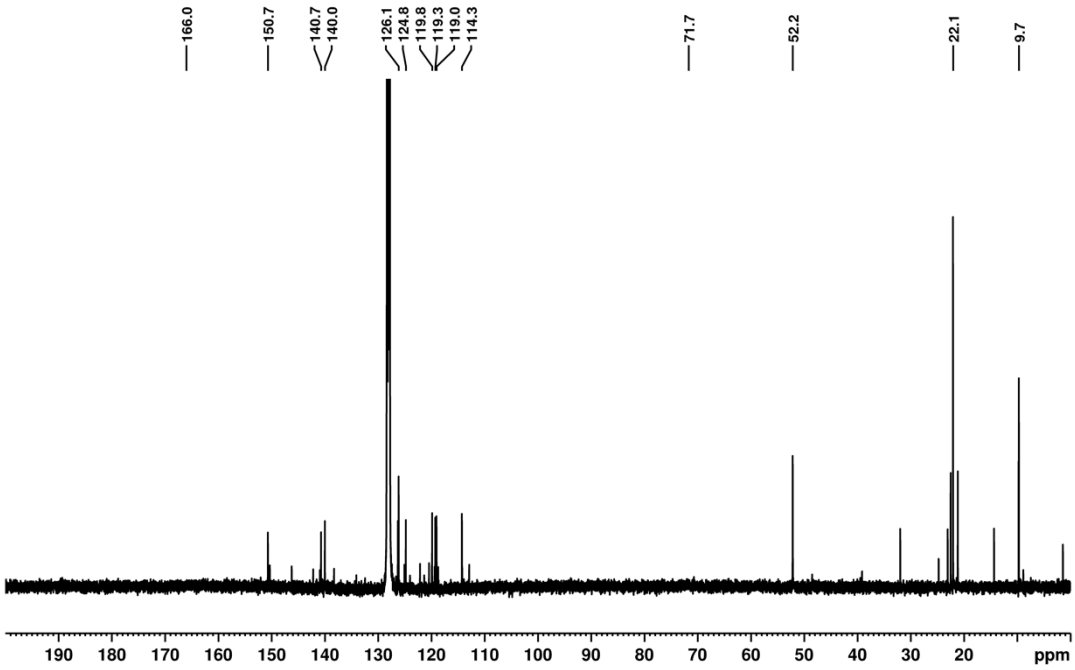

Figure S59. ^{13}C NMR spectrum (100.6 MHz, C_6D_6, 298 K) of {(I*i*Pr^{Me})·AlH-μ-Ind}$_2$ **22.**

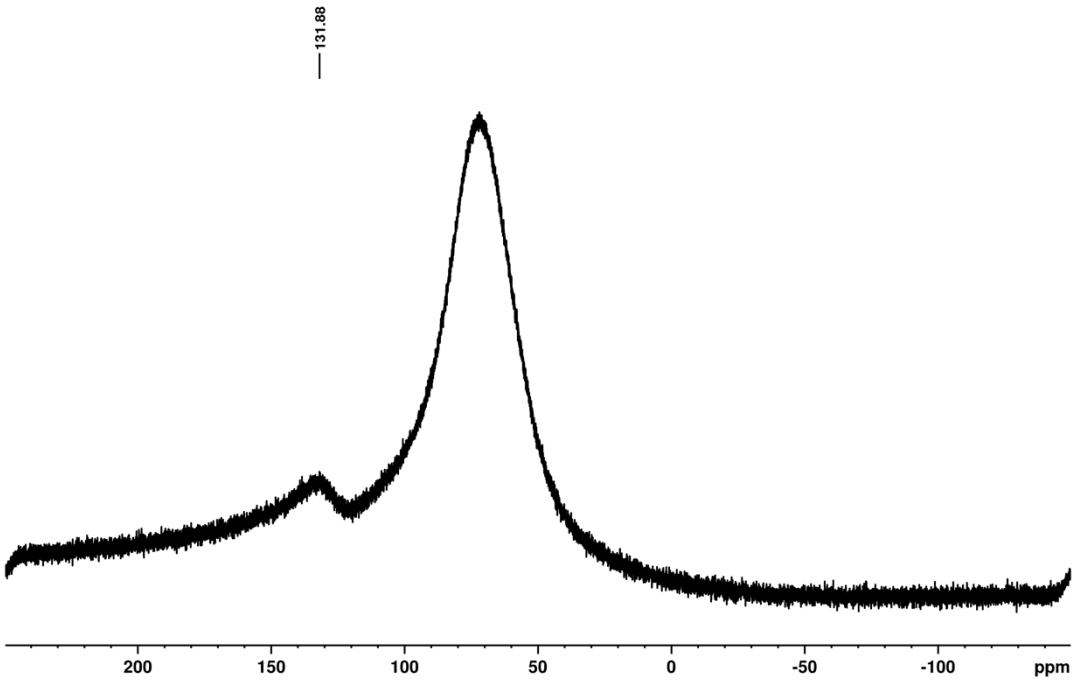

Figure S60. ^{27}Al NMR spectrum (104.3 MHz, C_6D_6, 298 K) of {(I*i*Pr^{Me})·AlH-μ-Ind}$_2$ **22**.

((IMe^{Me})·AlH-μ-Ind)$_3$ **23**:

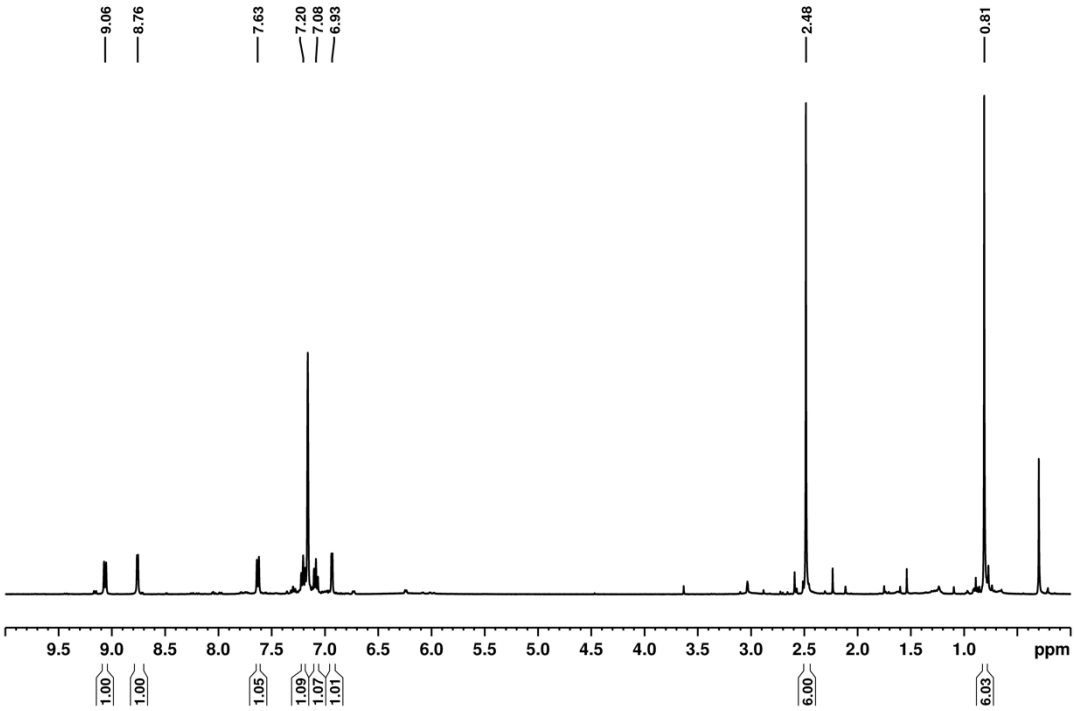

Figure S61. ^{1}H NMR spectrum (400.1 MHz, C_6D_6, 298 K) of {(IMe^{Me})·AlH-μ-Ind}$_3$ **23.**

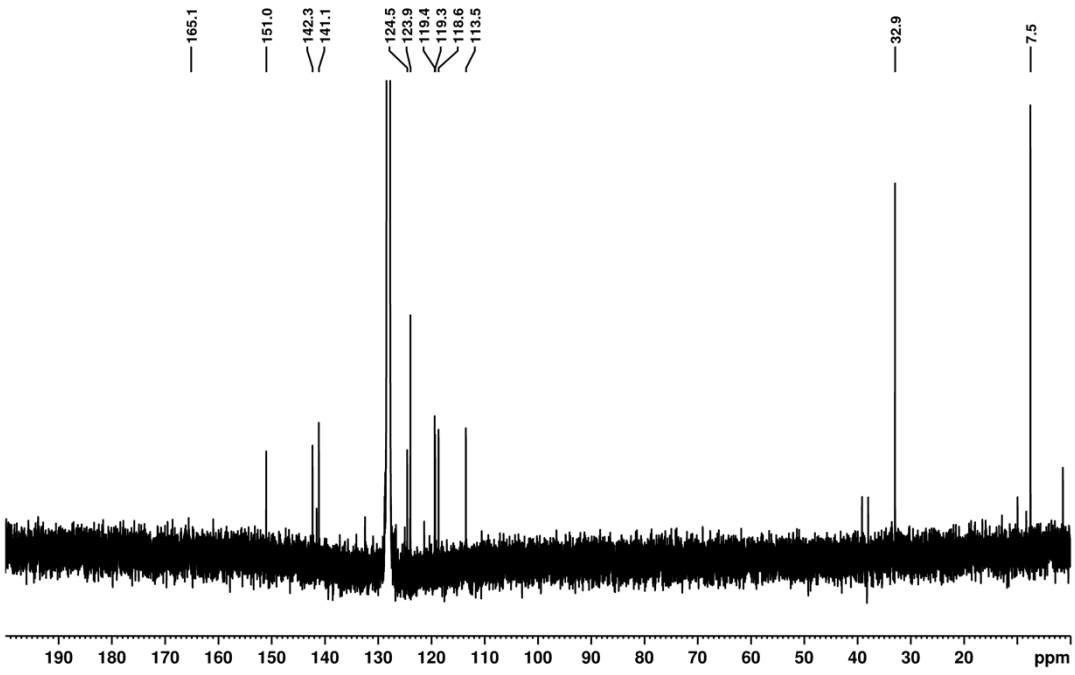

Figure S62. ^{13}C NMR spectrum (100.6 MHz, C_6D_6, 298 K) of {(IMe^{Me})·AlH-μ-Ind}$_3$ **23.**

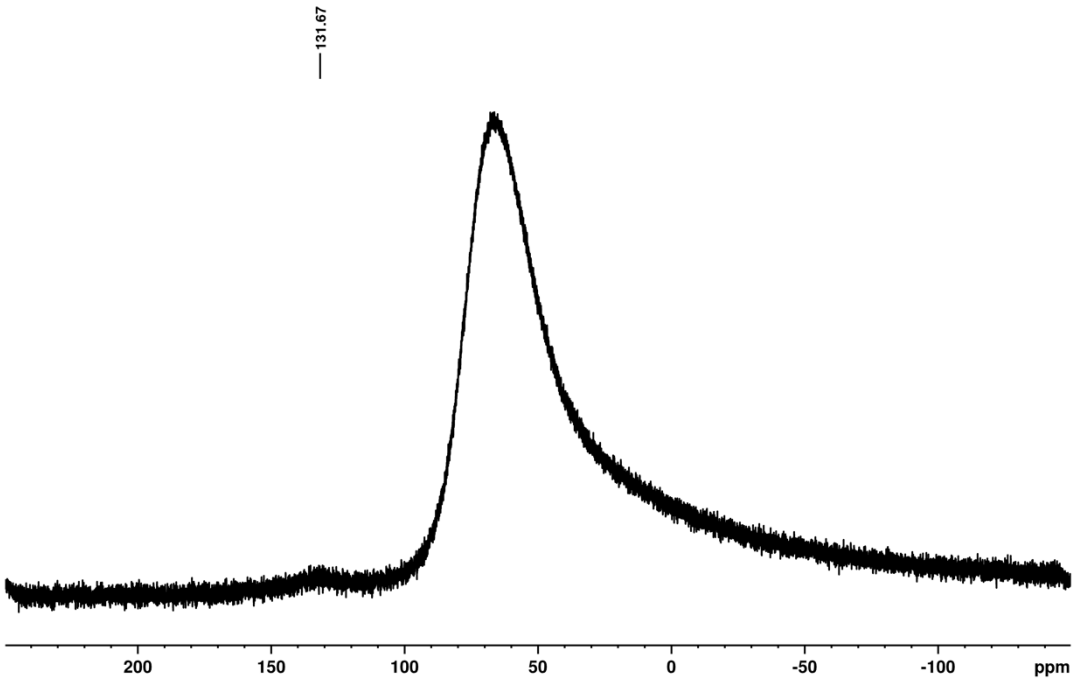

Figure S63. ^{27}Al NMR spectrum (104.3 MHz, C_6D_6, 298 K) of {(IMe^{Me})·AlH-μ-Ind}$_3$ **23**.

2) Thermal properties

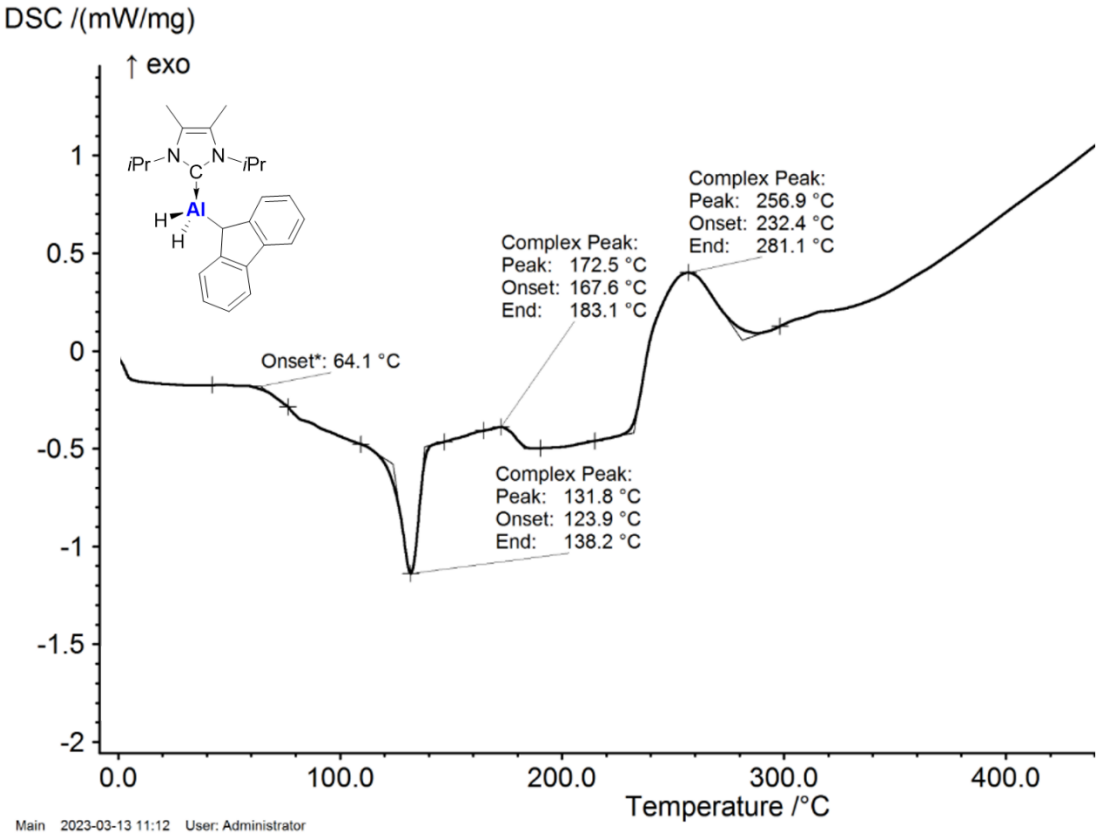

Figure S64. DSC curve of (I*i*Pr^{Me})·AlH$_2$Fl **4**.

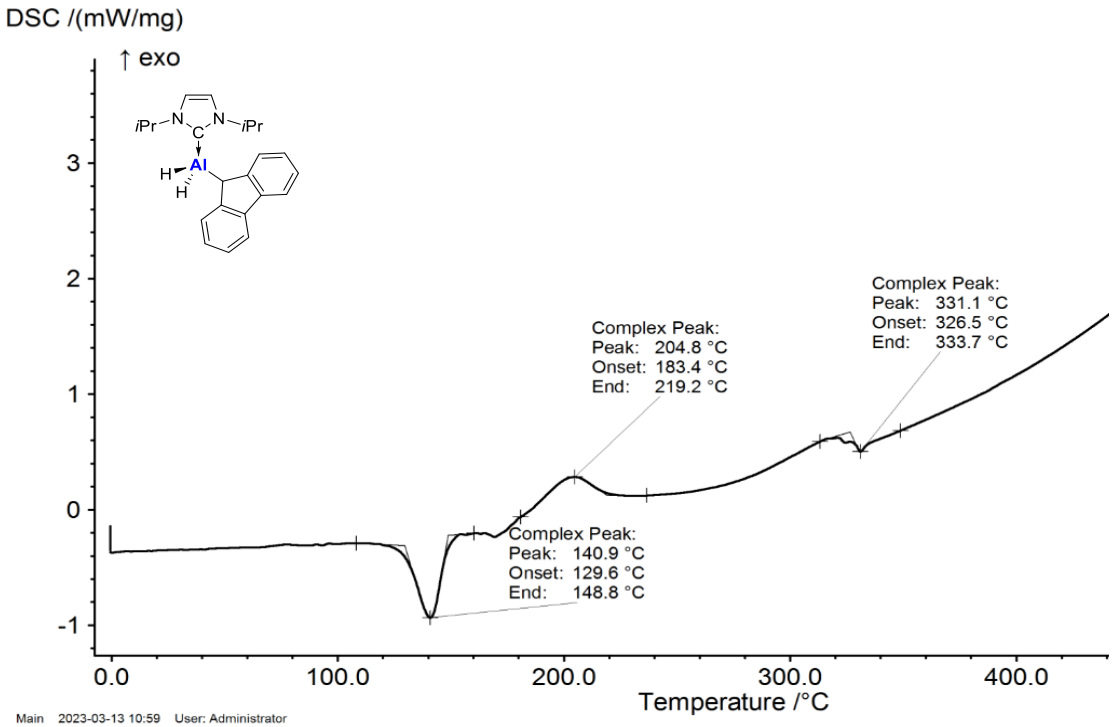

Figure S65. DSC curve of (I*i*Pr)·AlH$_2$Fl **5**

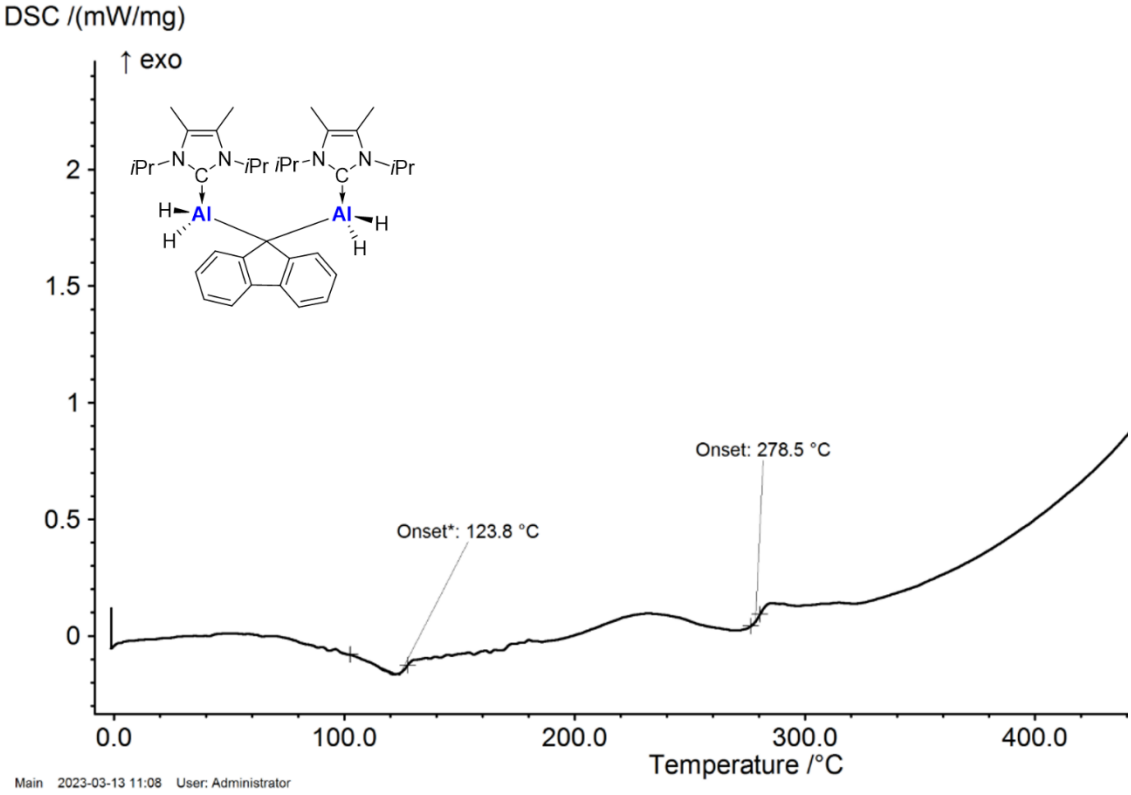

Figure S66. DSC curve of {(I*i*Pr^{Me})·AlH_2}$_2$-μ-Fl **19**

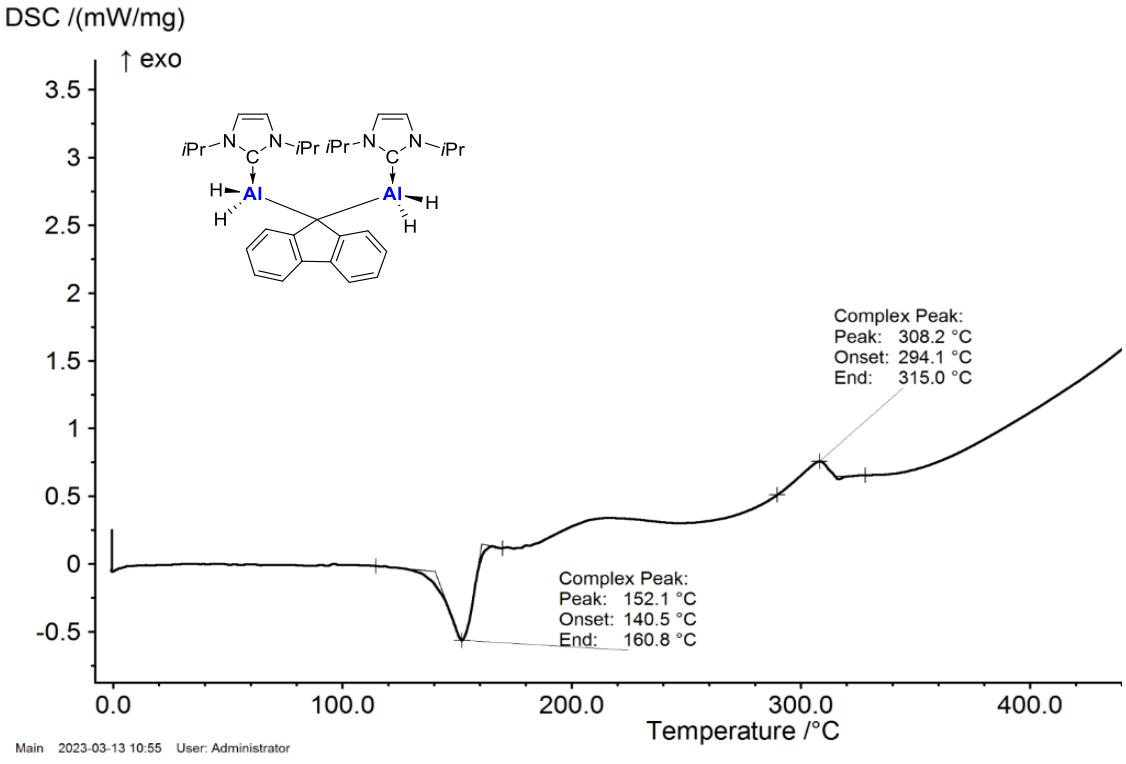

Figure S67. DSC curve of {(I*i*Pr)·AlH_2}$_2$-μ-Fl **20**

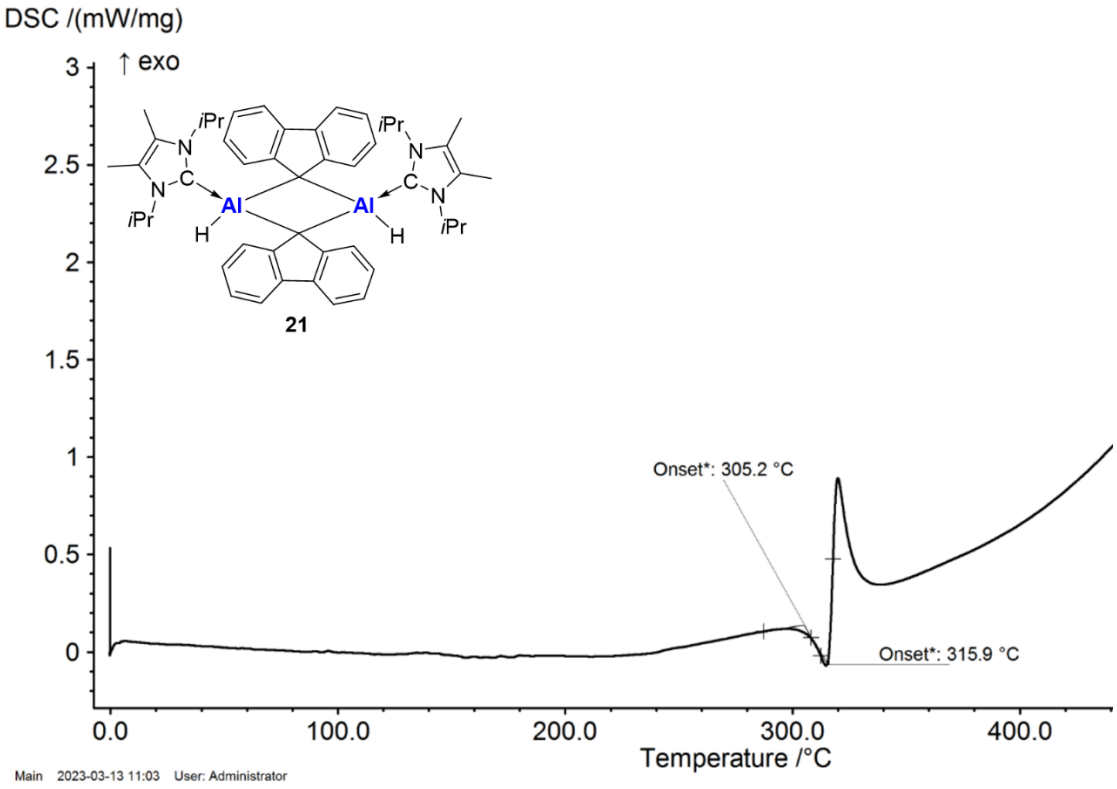

Figure S67. DSC curve of {(I*i*Pr)·AlH_2}$_2$-μ-Fl **20**

3) Crystal data collection and processing parameters

Crystal data collection and processing parameters are given in Table SI1. Crystals were immersed in a film of perfluoropolyether oil on a glass fiber MicroMountTM (MiTeGen) and transferred to a Bruker D8 Apex-1 diffractometer with CCD area detector and graphite-monochromated Mo-Kα radiation or a Bruker D8 Apex-2 diffractometer with CCD area detector and graphite-monochromated Mo-Kα radiation equipped with an Oxford Cryosystems low-temperature device or a Rigaku XtaLAB Synergy-DW diffractometer with HyPix-6000HE detector and monochromated Cu-Kα equipped with an Oxford Cryo 800 cooling unit. Data were collected at 100 K. The images were processed with the Bruker or Crysalis software packages and equivalent reflections were merged. Corrections for Lorentz-polarization effects and absorption were performed if necessary and the structures were solved by direct methods. Subsequent difference Fourier syntheses revealed the positions of all other non-hydrogen atoms. The structures were solved by using the ShelXTL software package.[S2] All non-hydrogen atoms were refined anisotropically. Hydrogen atoms were usually assigned to idealized positions and were included in structure factors calculations.

Table S1 Crystallographic data

	(IMe^{Me}) AlH$_2$Ind (3)	**(I*i*Pr^{Me}) AlH$_2$Fl (4)**	**(I*i*Pr) AlH$_2$Fl (5)**
Chemical formula	$C_{16}H_{21}AlN$	$C_{37}H_{41}AlN_2$	$C_{22}H_{27}AlN_2$
Formula Mass [g·mol^{-1}]	268.33	540.70	346.45
Temperature [K]	100(2)	100(2)	100(2)
Wavelength [Å]	1.54184	1.54184	1.54184
Crystal system	Triclinic	Monoclinic	Monoclinic
Space group	P-1	$P2_1/n$	$P2_1/c$
a [Å]	8.3243(2)	15.98870(10)	13.0917(2)
b [Å]	9.3597(3)	10.23650(10)	8.51850(10)
c [Å]	10.9459(3)	19.4053(2)	19.1232(3)
α [°]	110.610(2)	90	90
β [°]	100.206(2)	108.3190(10)	108.315(2)
γ [°]	103.225(2)	90	90
Unit cell volume [Å^3]	745.34(4)	3015.07(5)	2024.62(5)
No. of formula units per unit cell	2	4	4
Density (calc) [g·cm^{-3}]	1.196	1.191	1.137
Absorption coefficient [mm^{-1}]	1.078	0.785	0.901
F (000)	288	1160	744
Theta range ϑ [°]	4.499 to 77.571	3.137 to 77.717	3.556 to 77.557
Reflections collected	14601	115315	39939
Independent reflections	3083	6386	4270
Completeness to theta [%]	99.4	100	99.9
R_{int}	0.0429	0.0434	0.0524
Data	3083	6386	4270
Restraints	0	0	0
Parameter	184	375	238
*R*1 und *wR*2 for [$I > 2\sigma(I)$]	0.0433, 0.1143	0.0367, 0.0934	0.0449, 0.1283
*R*1 und *wR*2 (all data)	0.0489, 0.1181	0.0391, 0.0952	0.0490, 0.1325
Largest diff. peak and hole [eÅ^{-3}]	0.443 / -0.262	0.267 / -0.250	0.558 / -0.346
GooF	1.055	1.063	1.078
CCDC number	2328368	2328362	2328365

	(IMe^{Me}) AlH$_2$Fl (6)	**(I*i*Pr) GaH$_2$Ind (8)**	**(I*i*Pr) GaH$_2$Fl (11)**
Chemical formula	$C_{20}H_{23}AlN_2$	$C_{18}H_{25}GaN_2$	$C_{22}H_{27}GaN_2$
Formula Mass [g·mol^{-1}]	318.38	339.12	389.17
Temperature [K]	100(2)	100(2)	100(2)
Wavelength [Å]	1.54184	1.54184	1.54184
Crystal system	Orthorhombic	Orthorhombic	Monoclinic
Space group	$P2_12_12_1$	Pbca	$P2_1/c$
a [Å]	8.4966(2)	12.3946(2)	13.0769(5)
b [Å]	13.6726(3)	16.3096(2)	8.4982(2)
c [Å]	15.2417(3)	33.9295(5)	19.2047(8)
α [°]	90	90	90
β [°]	90	90	108.432(4)
γ [°]	90	90	90
Unit cell volume [Å^3]	1770.64(7)	6858.88(17)	2024.73(13)
No. of formula units per unit cell	4	16	4
Density (calc) [g·cm^{-3}]	11.194	1.314	1.277
Absorption coefficient [mm^{-1}]	0.989	2.139	1.365
F (000)	680	2848	816
Theta range ϑ [°]	4.344 to 77.485	2.605 to 73.952	2.236 to 31.097
Reflections collected	10475	47453	24227
Independent reflections	3464	6884	5348
Completeness to theta [%]	99.9	99.8	100
R_{int}	0.0404	0.0399	0.0388
Data	3464	6884	5348
Restraints	0	0	0
Parameter	220	403	238
*R*1 und *wR*2 for [$I > 2\sigma(I)$]	0.0358, 0.0909	0.0384, 0.041	0.0317, 0.0674
*R*1 und *wR*2 (all data)	0.0385, 0.0927	0.0518, 0.1007	0.0475, 0.0714
Largest diff. peak and hole [eÅ^{-3}]	0.175 / -0.296	1.080 / -0.665	0.401 / -0.308
GooF	1.066	1.021	1.049
CCDC number	2328363	2328357	2328366

	(IMe^{Me}) GaH_2Fl (12)	**($IiPr$) $AlHInd_2$ (14)**	**(IMe^{Me}) $AlHInd_2$ (15)**
Chemical formula	$C_{20}H_{23}GaN_2$	$C_{27}H_{31}AlN_2$	$C_{25}H_{27}AlN_2$
Formula Mass [g·mol^{-1}]	361.12	410.52	382.46
Temperature [K]	100(2)	100.(2)	100(2)
Wavelength [Å]	1.54184	1.54184	1.54184
Crystal system	Orthorhombic	Monoclinic	Monoclinic
Space group	$P2_12_12_1$	$P2_1/c$	$P2_1/n$
a [Å]	8.4828(2)	8.6951(2)	12.2976(2)
b [Å]	13.6588(5)	12.8561(2)	11.66710(10)
c [Å]	15.2488(5)	20.8697(3)	15.7205(2)
α [°]	90	90	90
β [°]	90	101.996(2)	107.158(2)
γ [°]	90	90	90
Unit cell volume [Å^3]	1766.80(10)	2281.97(7)	2155.15(5)
No. of formula units per unit cell	4	4	4
Density (calc) [g·cm^{-3}]	1.358	1.195	1.179
Absorption coefficient [mm^{-1}]	2.117	0.879	0.897
F (000)	752	880	816
Theta range ϑ [°]	4.346 to 77.906	4.064 to 80.346	4.035 to 79.834
Reflections collected	10282	13412	22682
Independent reflections	3486	4614	4602
Completeness to theta [%]	99.9	96.2	100
R_{int}	0.0444	0.0460	0.0378
Data	3486	4614	4602
Restraints	0	0	281
Parameter	218	279	346
*R*1 und *wR*2 for [$I > 2\sigma(I)$]	0.0380, 0.0961	0.0434, 0.1083	0.0403, 0.1046
*R*1 und *wR*2 (all data)	0.0400, 0.0971	0.0539, 0.1142	0.0444, 0.1070
Largest diff. peak and hole [eÅ^{-3}]	0.607 / -0.461	0.258 / -0.302	0.270 / -0.252
GooF	1.079	1.070	1.047
CCDC number	2328355	2328370	2328360

	(I*i*Pr^{Me}) AlHFl$_2$ (16)	**(IMe^{Me}) AlHFl$_2$ (18)**	**{(I*i*Pr^{Me}) AlH$_2$}$_2$-Fl (19)**
Chemical formula	$C_{43}H_{45}AlN_2$	$C_{33}H_{31}AlN_2$	$C_{35}H_{52}Al_2N_4$
Formula Mass [g·mol^{-1}]	616.79	482.58	582.76
Temperature [K]	100(2)	100(2)	100(2)
Wavelength [Å]	1.54184	1.54184	1.54184
Crystal system	Triclinic	Triclinic	Monoclinic
Space group	P1	P-1	I2/a
a [Å]	9.7049(2)	12.14390(10)	17.5752(3)
b [Å]	10.1111(2)	13.0413(2)	10.5232(2)
c [Å]	10.2297(2)	16.6824(2)	38.6355(8)
α [°]	96.7320(10)	82.0080(10)	90
β [°]	103.215(2)	88.6270(10)	98.272(2)
γ [°]	114.685(2)	84.5490(10)	90
Unit cell volume [Å^3]	861.88(3)	2604.38(6)	7071.2(2)
No. of formula units per unit cell	1	4	8
Density (calc) [g·cm^{-3}]	1.188	1.231	1.095
Absorption coefficient [mm^{-1}]	0.750	0.853	0.940
F (000)	330	1024	2528
Theta range ϑ [°]	4.574 to 77.034	2.675 to 77.701	2.311 to 74.325
Reflections collected	18147	53139	37833
Independent reflections	5069	10928	7062
Completeness to theta [%]	99.8	100	99.8
R_{int}	0.0258	0.0426	0.0307
Data	5096	10928	7062
Restraints	3	0	0
Parameter	425	665	398
*R*1 und *wR*2 for [$I > 2\sigma(I)$]	0.0278, 0.0739	0.0386, 0.0957	0.0545, 0.1298
*R*1 und *wR*2 (all data)	0.0282, 0.0743	0.0442, 0.0991	0.0654, 0.1359
Largest diff. peak and hole [eÅ^{-3}]	0.191 / -0.208	0.304 / -0.270	0.700 / -0.285
GooF	1.036	1.022	1.073
CCDC number	2328364	2328358	2328361

	{(l*i*Pr) AlH_2}$_2$-Fl (20)	**{(l*i*Pr^{Me}) AlHFl}$_2$ (21)**	**{(l*i*Pr^{Me}) AlHInd}$_2$ (22)**
Chemical formula	$C_{31}H_{44}Al_2N_4$	$C_{48}H_{58}Al_2N_4$	$C_{43}H_{61}Al_2N_4$
Formula Mass [g·mol^{-1}]	526.66	744.94	687.91
Temperature [K]	100(2)	100(2)	100(2)
Wavelength [Å]	1.54184	1.54184	1.54184
Crystal system	Monoclinic	Monoclinic	Monoclinic
Space group	$P2_1/c$	$P2_1/c$	$P2_1/n$
a [Å]	19.1995(5)	12.6278(2)	13.53080(10)
b [Å]	10.24520(10)	16.1570(2)	14.21250(10)
c [Å]	17.0700(3)	21.6852(4)	21.8135(2)
α [°]	90	90	90
β [°]	114.130(3)	106.420(2)	97.1080(10)
γ [°]	90	90	90
Unit cell volume [Å^3]	3064.32(12)	4243.93(12)	4162.64(6)
No. of formula units per unit cell	4	4	4
Density (calc) [g·cm^{-3}]	1.142	1.166	1.098
Absorption coefficient [mm^{-1}]	1.037	0.894	0.868
F (000)	1136	1600	1492
Theta range ϑ [°]	5.001 to 67.078	3.464 to 77.656	3.653 to 80.074
Reflections collected	16241	23665	43459
Independent reflections	5253	8214	8875
Completeness to theta [%]	96	96	99.8
R_{int}	0.0398	0.0267	0.0836
Data	5253	8214	8875
Restraints	0	0	0
Parameter	358	507	463
*R*1 und *wR*2 for [$I > 2\sigma(I)$]	0.0548, 0.1540	0.0400, 0.1063	0.0555, 0.1538
*R*1 und *wR*2 (all data)	0.0728, 0.1661	0.0479, 0.1117	0.0594, 0.1579
Largest diff. peak and hole [eÅ^{-3}]	0.501 / -0.407	0.395 / -0.303	1.087 / -0.464
GooF	1.055	1.065	1.066
CCDC number	2328369	2328367	2328356

	{(IMe^{Me}) AlHInd}$_3$ (23)
Chemical formula	$C_{55}H_{65}Al_3N_6$
Formula Mass [g·mol^{-1}]	891.07
Temperature [K]	100(2)
Wavelength [Å]	1.54184
Crystal system	Triclinic
Space group	P-1
a [Å]	8.3610(2)
b [Å]	16.6235(5)
c [Å]	18.8508(4)
α [°]	100.766(2)
β [°]	99.620(2)
γ [°]	92.091(2)
Unit cell volume [Å^3]	2531.53(11)
No. of formula units per unit cell	2
Density (calc) [g·cm^{-3}]	1.169
Absorption coefficient [mm^{-1}]	1.002
F (000)	952
Theta range ϑ [°]	2.712 to 80.172
Reflections collected	40506
Independent reflections	10540
Completeness to theta [%]	98.6
R_{int}	0.1009
Data	10540
Restraints	79
Parameter	628
*R*1 und *wR*2 for [$I > 2\sigma(I)$]	0.0884, 0.2099
*R*1 und *wR*2 (all data)	0.1185, 0.2249
Largest diff. peak and hole [eÅ^{-3}]	0.741 / -0.547
GooF	1.093
CCDC number	2328359

References:

[S1] For a discussion of these equilibria for cyclopentadienyl compounds see: L. Werner, S. Mann, Udo Radius, *Eur. J. Inorg. Chem.* 2023, e202300398

[S2] G. M. Sheldrick, *Acta Crystallogr., Sect. A: Found. Adv* 2014, **70**, C1437.